NASA Technical Memorandum 103900

The Asymptotic Spectra of Banded Toeplitz and Quasi-Toeplitz Matrices

Richard M. Beam and Robert F. Warming, Ames Research Center, Moffett Field, California.

November 1991

National Aeronautics and
Space Administration

Ames Research Center
Moffett Field, California 94035-1000

THE ASYMPTOTIC SPECTRA OF BANDED TOEPLITZ AND QUASI-TOEPLITZ MATRICES[1]

RICHARD M. BEAM AND ROBERT F. WARMING

NASA AMES RESEARCH CENTER, MOFFETT FIELD, CA 94035, USA

Abstract. Toeplitz matrices occur in many mathematical as well as scientific and engineering investigations. This paper considers the spectra of *banded* Toeplitz and *quasi*-Toeplitz matrices with emphasis on non-normal matrices of arbitrarily large order and relatively small bandwidth. These are the type of matrices that appear in the investigation of stability and convergence of difference approximations to partial differential equations. Quasi-Toeplitz matrices are the result of non-Dirichlet boundary conditions for the difference approximations. The eigenvalue problem for a banded Toeplitz or quasi-Toeplitz matrix of large order is, in general, analytically intractable and (for non-normal matrices) numerically unreliable. An asymptotic (matrix order approaches infinity) approach partitions the eigenvalue analysis of a quasi-Toeplitz matrix into two parts, namely the analysis for the boundary condition *independent* spectrum and the analysis for the boundary condition *dependent* spectrum. The boundary condition independent spectrum is the same as the *pure* Toeplitz matrix spectrum. Algorithms for computing both parts of the spectrum are presented. Examples are used to demonstrate the utility of the algorithms, to present some interesting spectra, and to point out some of the numerical difficulties encountered when conventional matrix eigenvalue routines are employed for non-normal matrices of large order. The analysis for the Toeplitz spectrum also leads to a diagonal similarity transformation that improves conventional numerical eigenvalue computations. Finally, the algorithm for the asymptotic spectrum is extended to the Toeplitz generalized eigenvalue problem which occurs, for example, in the stability analysis of Padé type difference approximations to differential equations.

Key words. Toeplitz matrices, eigenvalues, spectrum, stability

AMS(MOS) subject classifications. 65F15,65M10,76N10

1. Introduction. A Toeplitz matrix has the property that the entries are constant along diagonals parallel to the main diagonal. If we define the sequence

$$a_{-p}, a_{-p+1}, \cdots, a_0, \cdots, a_{q-1}, a_q; \quad \text{where} \quad a_{-p}, a_q \neq 0 \tag{1.1}$$

and p and q are specified positive integers, then the elements of a *banded* square Toeplitz matrix of order J and bandwidth $p+q+1(\leq J)$ are given by

$$a_{ij} = a_{j-i} \tag{1.2}$$

if a_{j-i} is a member of the sequence (1.1) and zero otherwise. Since the eigenvalue analysis for triangular matrices is trivial, we have restricted our attention to *non*-triangular matrices

[1] The main results of this paper were presented at the 14th Biennial Conference on Numerical Analysis, Dundee, Scotland, June 25 to 28, 1991.

$(p, q > 0)$. For example, if we choose $p = 1$ and $q = 2$ and denote the banded Toeplitz matrix by $\mathbf{A}$ then

$$\mathbf{A} = \begin{bmatrix} a_0 & a_1 & a_2 & & & & & & \\ a_{-1} & a_0 & a_1 & a_2 & & & & & \\ & a_{-1} & a_0 & a_1 & a_2 & & O & & \\ & & \cdot & \cdot & \cdot & \cdot & & & \\ & & & \cdot & \cdot & \cdot & \cdot & & \\ & & & & \cdot & \cdot & \cdot & \cdot & \\ & & O & & & a_{-1} & a_0 & a_1 & a_2 \\ & & & & & & a_{-1} & a_0 & a_1 \\ & & & & & & & a_{-1} & a_0 \end{bmatrix} \tag{1.3}$$

where the bandwidth is 4 and the matrix order J is arbitrary. Our interest is in the spectra, i.e., the eigenvalues, for banded Toeplitz matrices of arbitrarily large order.

A banded *quasi*-Toeplitz matrix is defined to be a banded Toeplitz matrix where there are a limited number of row changes constrained as follows: There are at most p altered rows among the first p rows and at most q altered rows among the last q rows. Since p and q are fixed and J is assumed to be large, there are only a relatively few altered rows. Here we use *quasi* in the conventional sense meaning *almost* or *nearly*. For example, a quasi-Toeplitz cousin of the Toeplitz matrix (1.3) is

$$\mathbf{A} = \begin{bmatrix} b_{11} & b_{12} & b_{13} & b_{14} & & & & & \\ a_{-1} & a_0 & a_1 & a_2 & & & & & \\ & a_{-1} & a_0 & a_1 & a_2 & & O & & \\ & & \cdot & \cdot & \cdot & \cdot & & & \\ & & & \cdot & \cdot & \cdot & \cdot & & \\ & & & & \cdot & \cdot & \cdot & \cdot & \\ & & O & & & a_{-1} & a_0 & a_1 & a_2 \\ & & & & & c_{24} & c_{23} & c_{22} & c_{21} \\ & & & & & c_{14} & c_{13} & c_{12} & c_{11} \end{bmatrix}. \tag{1.4}$$

(The advantage of the unusual indexing for the c entries of $\mathbf{A}$ will become apparent in Section 4.2). We assume that the modified elements are constants and therefore independent of J. The bandwidth of a quasi-Toeplitz matrix may be larger than the bandwidth of its pure Toeplitz cousin, e.g., the quasi-Toeplitz matrix defined by (1.4) has a larger bandwidth than its Toeplitz cousin defined by (1.3).

Another important relative of a banded Toeplitz matrix is its *circulant* cousin. Each row of a circulant matrix is constructed by cycling the previous row forward one element. For example, if the first row of a matrix of order J is

$$[a_0, a_1, \cdots, a_q, 0, \cdots, 0, a_{-p}, \cdots, a_{-2}, a_{-1}]. \tag{1.5}$$

this process defines the circulant cousin of the Toeplitz matrix defined by (1.2). In partic-

ular, the circulant cousin of the Toeplitz matrix (1.3) is

$$\mathbf{A} = \begin{bmatrix} a_0 & a_1 & a_2 & & & & & a_{-1} \\ a_{-1} & a_0 & a_1 & a_2 & & & & \\ & a_{-1} & a_0 & a_1 & a_2 & & O & \\ & & \cdot & \cdot & \cdot & \cdot & & \\ & & & \cdot & \cdot & \cdot & \cdot & \\ & & & & \cdot & \cdot & \cdot & \cdot \\ & & O & & & a_{-1} & a_0 & a_1 & a_2 \\ a_2 & & & & & & a_{-1} & a_0 & a_1 \\ a_1 & a_2 & & & & & & a_{-1} & a_0 \end{bmatrix}. \tag{1.6}$$

We will also refer to the matrix defined by (1.5) as the circulant cousin of the quasi-Toeplitz matrix, e.g., (1.6) is the circulant cousin of (1.4). A circulant matrix is also Toeplitz because the entries are constant along diagonals. The eigenvalues (and eigenvectors) of any circulant matrix can be determined analytically [1]. The spectrum for a circulant banded Toeplitz matrix is a subset of the spectrum for the doubly infinite (order) banded Toeplitz matrix [9].

Toeplitz matrices are important in mathematics as well as scientific and engineering applications [5,4]. Our interest [14] arose from an investigation of stability and convergence of difference approximations to initial-boundary-value problems for partial differential equations. The analysis of these difference approximations leads to a study of the spectra for banded quasi-Toeplitz matrices of large order. The element changes from the pure Toeplitz matrix are the result of applying non-Dirichlet boundary conditions to the difference equations. The bandwidth of the matrix is determined by the width of the difference stencil and is small compared with the order of the matrix. For example, if the method of lines is applied to a scalar hyperbolic partial differential equation and if a four point spatial difference approximation is used to approximate the spatial derivative, the stability analysis matrix is the quasi-Toeplitz matrix:

$$\begin{bmatrix} -\frac{2\alpha+3}{2} & 3\alpha+2 & -\frac{6\alpha+1}{2} & \alpha & & & & & \\ -\frac{1}{3} & -\frac{1}{2} & 1 & -\frac{1}{6} & & & & & \\ & -\frac{1}{3} & -\frac{1}{2} & 1 & -\frac{1}{6} & & O & & \\ & & \cdot & \cdot & \cdot & \cdot & & & \\ & & & \cdot & \cdot & \cdot & \cdot & & \\ & & & & \cdot & \cdot & \cdot & \cdot & \\ & & O & & & -\frac{1}{3} & -\frac{1}{2} & 1 & -\frac{1}{6} \\ & & & & & & -\frac{1}{3} & -\frac{1}{2} & 1 \\ & & & & & & -\beta & \frac{6\beta-1}{2} & -3\beta \end{bmatrix} \tag{1.7}$$

where the parameters α and β are introduced by the numerical boundary conditions [14]. If we choose $\alpha = 6/5$ and $\beta = -4/5$ and calculate the spectrum of (1.7) for a sequence of increasing matrix orders, we obtain the spectra shown by the open circles in the complex plane in Fig. 1.1. (The abscissa and the ordinate of each eigenvalue, respectively, represent the real part and the imaginary part of the eigenvalue.) In the stability analysis of a

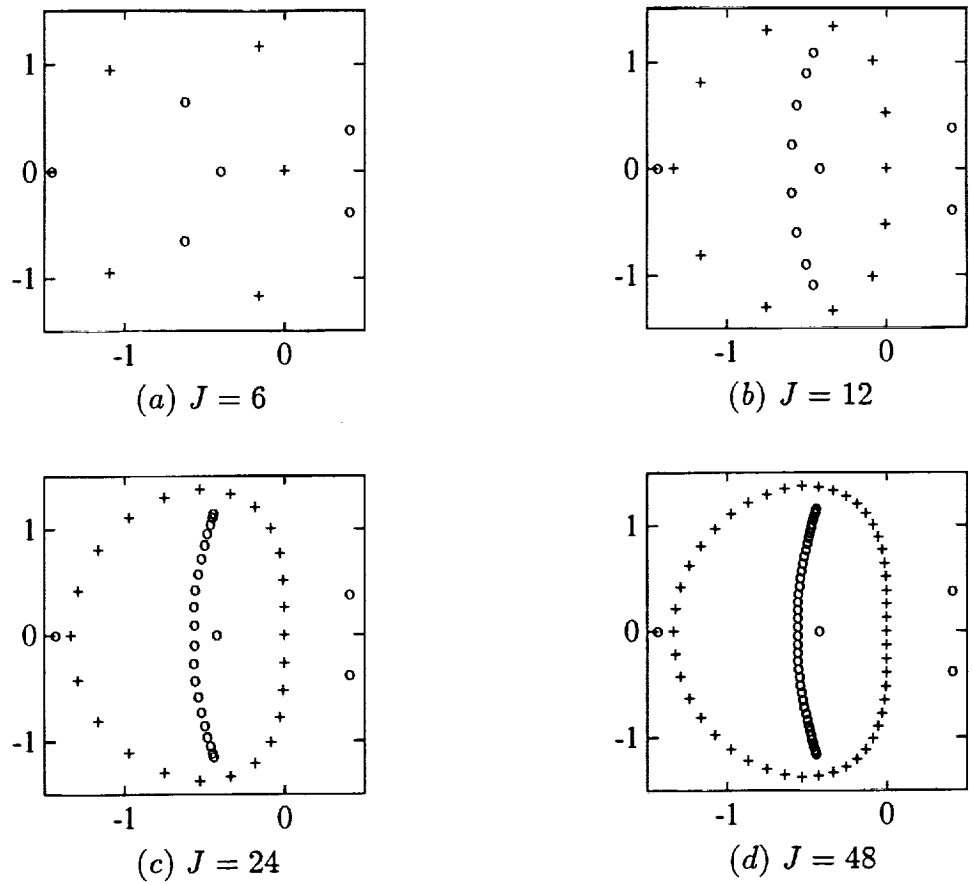

FIGURE 1.1. *Numerically computed spectra for the quasi-Toeplitz matrix (1.7), with* $\alpha = 6/5$ *and* $\beta = -4/5$, *(o symbol) and the analytically computed spectra for the circulant Toeplitz cousin (+ symbol) for matrix order* J.

difference method (and for the purposes of this paper) we are interested in the spectrum for large (approaching infinity) matrix order, e.g., Fig. 1.1d. For reference we have plotted the spectrum for the circulant cousin of (1.7) in Fig. 1.1. The circulant spectrum is indicated by the + symbols.

In Section 2 the eigenvalue problem for a banded Toeplitz or quasi-Toeplitz matrix is formulated as a difference equation with appropriate boundary conditions. In general, the resulting boundary value problem is analytically intractable. In Section 3 we assume that the order of a quasi-Toeplitz matrix is large and use an asymptotic approach to partition the eigenvalues into two independent groups. The partition is between boundary condition *independent* eigenvalues and boundary condition *dependent* eigenvalues. Algorithms for the computation of both parts of the spectrum are described in Section 4. These algorithms involve the solution of algebraic equations with degree proportional to the bandwidth of the matrix. The algorithm for the boundary condition dependent spectrum closely parallels the eigenvalue analysis of Godunov and Ryabenkii [2], Kreiss [7] and Gustafsson, Kreiss, and Sundström [6]. Plots of the spectra of Toeplitz matrices often exhibit surprising

geometrical shapes. Some illustrative examples are shown in Section 5. The algorithms for computing the spectra are applied to both Toeplitz and quasi-Toeplitz matrices in Section 6. If conventional numerical eigenvalue algorithms are used to compute the spectra for non-normal matrices of large order, errors in the spectra may be encountered. In Section 7 we introduce a simple similarity transformation that improves the accuracy of conventional eigenvalue algorithms for a large class of banded Toeplitz and quasi-Toeplitz matrices. Finally, the Toeplitz eigenvalue algorithm is extended to the generalized eigenvalue problem in Section 8.

2. The eigenvalue problem: a difference equation representation. Let $\mathbf{A}$ represent a $J \times J$ banded Toeplitz matrix defined by (1.2). The eigenvalue problem for $\mathbf{A}$ is defined by

$$\mathbf{A}\boldsymbol{\phi} = \lambda\boldsymbol{\phi} \tag{2.1}$$

where $\boldsymbol{\phi}$ is the eigenvector and λ is the eigenvalue. The indexing of the eigenvector $\boldsymbol{\phi}$ is arbitrary and we choose

$$\boldsymbol{\phi}^T = [\phi_1, \phi_2, \cdots, \phi_{J-1}, \phi_J]. \tag{2.2}$$

The eigenvalue problem (2.1) is equivalent to the system of homogeneous difference equations

$$\sum_{m=-p}^{q} a_m \phi_{j+m} = \lambda\phi_j, \quad j = 1, 2, \cdots, J \tag{2.3}$$

with p homogeneous Dirichlet boundary conditions at the left boundary and q homogeneous boundary conditions at the right boundary :

$$\phi_{-m} = 0, \quad m = 0, 1, \cdots, p-1, \qquad \phi_{J+m} = 0, \quad m = 1, 2, \cdots, q. \tag{2.4a,b}$$

Note that fictitious points have been introduced in defining the boundary conditions (2.4). It is apparent that (2.3) is the generic equation of the system (2.1).

Each of the equations (2.3) is a $(p+q)$-th order difference equation for ϕ_j and we look for a solution of the form

$$\phi_j = \kappa^j \tag{2.5}$$

where κ is a complex constant. Insertion of (2.5) into (2.3) yields

$$\lambda = \sum_{m=-p}^{q} a_m \kappa^m. \tag{2.6}$$

This is an algebraic equation of degree $p+q$ in the unknown κ and in the following analysis we assume the roots are distinct. The general solution of (2.3) is

$$\phi_j = \sum_{m=1}^{p+q} \beta_m \kappa_m^j \tag{2.7}$$

where the κ_m's are the roots of (2.6) and the β_m's are arbitrary constants. The constants β_m are determined by inserting (2.7) into the boundary conditions (2.4). If the bandwidth is three, i.e., $p = q = 1$, the eigenvalue problem for the pure Toeplitz problem can be solved analytically [10,15]. However, if the bandwidth is greater than three, the problem is analytically intractable.

For a quasi-Toeplitz matrix the difference equation formulation of the eigenvalue problem differs from the pure Toeplitz problem only in the boundary conditions. The difference equations (2.3) are still valid if appropriate extrapolation boundary conditions are generated. These extrapolation boundary conditions depend on the matrix entries that change the matrix from Toeplitz to quasi-Toeplitz. Extrapolation boundary conditions have the general form

$$\text{(2.8a,b)} \quad P_{-m}(E)\phi_{-m} = 0, \quad m = 0, 1, \cdots, p-1, \quad Q_m(E)\phi_{J+m} = 0, \quad m = 1, 2, \cdots, q$$

where $P_{-m}(E)$ and $Q_m(E)$ are polynomial operators and E is the shift operator defined by $E\phi_j = \phi_{j+1}$. The subscripts on the operators indicate that, in general, the operators are different for each value of m. As an example, the extrapolation boundary conditions for the matrix (1.7) are

$$\text{(2.9a,b,c)} \qquad P_0(E)\phi_0 = 0, \quad Q_1(E)\phi_{J+1} = 0, \quad Q_2(E)\phi_{J+2} = 0$$

where, after some algebra, one finds

$$\text{(2.10a,b,c)} \quad P_0(E) = (E-1)^3(3\alpha E - 1), \quad Q_1(E) = 1, \quad Q_2(E) = (1-E^{-1})^3(1+6\beta E^{-1}).$$

Although the extrapolation boundary conditions are easy to derive, we will find it more convenient to implement an eigenvalue algorithm which uses the boundary difference equations directly. For example, the first row and the last two rows of the matrix (1.4) have entry changes. For the eigenvalue problem (2.1) the difference equations (2.3) are still valid at $j = 2, 3, \cdots, J-2$ and modified difference equations apply at $j = 1, J-1, J$. The general form of difference equations for the *left* boundary is

$$\text{(2.11)} \qquad \mathbf{B}\tilde{\boldsymbol{\phi}} = \lambda \mathbf{D}\tilde{\boldsymbol{\phi}}$$

where $\mathbf{B}$ is a rectangular matrix with p rows and $r(\leq J)$ columns and $\tilde{\boldsymbol{\phi}}^T = [\phi_1, \phi_2, \cdots, \phi_r]$. The matrix $\mathbf{D}$ is a $p \times r$ rectangular diagonal matrix with unit entries on the diagonal. Similar equations apply at the right boundary.

The eigenvalue problem for the circulant cousin of (1.2) is (2.3) with periodic boundary conditions:

$$\text{(2.12)} \qquad \phi_j = \phi_{j+J}.$$

It is well-known that the eigenvalue problem for any circulant matrix can be solved analytically. By inserting (2.5) into (2.12), one obtains

$$\text{(2.13)} \qquad \kappa^J = 1.$$

Hence the κ's are the J roots of unity:

$$\kappa_\ell = e^{i\theta_\ell}, \quad \text{where} \quad \theta_\ell = 2\ell\pi/J, \quad \ell = 1, 2, \cdots, J. \tag{2.14}$$

The circulant spectrum is obtained by substituting (2.14) into (2.6):

$$\lambda_\ell = \sum_{m=-p}^{q} a_m e^{im\theta_\ell}. \tag{2.15}$$

As an example, the spectrum of the circulant matrix (1.6) with coefficients

$$[a_{-1}, a_0, a_1, a_2] = [-1/3, \underline{-1/2}, 1, -1/6] \tag{2.16}$$

reduces to the compact form:

$$\lambda_\ell = -4w_\ell^2/3 - i[1 + 2w_\ell/3] \sin\theta_\ell, \tag{2.17}$$

where

$$w_\ell = \sin^2(\theta_\ell/2), \quad \theta_\ell = 2\ell\pi/J, \quad \ell = 1, 2, \cdots, J. \tag{2.18}$$

The eigenvalue locus is the *oval* shaped dashed line plotted in Fig. 5.1. In equation (2.16) and the remainder of this paper we use the underline to indicate the main diagonal element.

3. Partition of the spectrum. If we assume that the order J of a quasi-Toeplitz matrix is large ($J \to \infty$) we can partition the eigenvalues into two groups. The partition is between (a) eigenvalues which are *independent* of the boundary conditions and (b) eigenvalues which are *dependent* on the boundary conditions. Group (b) may be empty.

We assume without loss of generality that the $p+q$ roots of the algebraic equation (2.6) are ordered as

$$|\kappa_1| \le |\kappa_2| \le \cdots \le |\kappa_p| \le |\kappa_{p+1}| \le \cdots \le |\kappa_{p+q}|. \tag{3.1}$$

It should be noted that each κ is a function of λ.

The crucial inequality in (3.1) is between $|\kappa_p|$ and $|\kappa_{p+1}|$. As $J \to \infty$ there are only two choices: either

$$|\kappa_p| = |\kappa_{p+1}| \qquad \text{or} \qquad |\kappa_p| < |\kappa_{p+1}|. \tag{3.2a,b}$$

This simple observation divides the asymptotic spectrum into two groups. In this section, we briefly describe the properties of the two groups. Schmidt and Spitzer [9] proved the equivalence of the eigenvalues associated with the κ's of (3.2a) and the asymptotic ($J \to \infty$) spectrum of the banded Toeplitz matrix.

We first consider the case of equality (3.2a):

(3.3) group (a): $$|\kappa_p| = |\kappa_{p+1}|.$$

For large J ($J \to \infty$), the κ's of equal modulus (3.3) couple the left and right boundaries for the eigenfunction given by (2.7). On the other hand, the equality (3.3) allows one to find the asymptotic spectrum which is *independent* of the boundary conditions. This may seem like a paradox, but the algorithmic details in the next section clarify how it is possible for the κ's and the spectrum to be independent of the boundary conditions.

Next we consider the inequality (3.2b):

(3.4) group (b): $$|\kappa_p| < |\kappa_{p+1}|.$$

In this case, the left and right boundaries are uncoupled for large J ($J \to \infty$). Furthermore, the corresponding eigenvalues are dependent on the boundary conditions. Eigenvalues in group (b) depend intimately on the choice of boundary conditions and for certain choices there will be no eigenvalues in this group. One choice of boundary conditions which introduces no eigenvalues of group (b) is the Dirichlet boundary conditions (2.4) (see, e.g.,Section 6.2). Since Dirichlet boundary conditions lead to a pure Toeplitz eigenvalue problem, we conclude that *the spectrum for a pure Toeplitz matrix is composed only of the boundary condition independent eigenvalues.*

4. Algorithms for computing the spectra. In this section we present algorithms for computing the asymptotic spectra of Toeplitz and quasi-Toeplitz matrices. We separate the algorithms according to the two groups of eigenvalues: (a) boundary condition independent (pure Toeplitz) and (b) boundary condition dependent. The application of each algorithm involves the solution of algebraic equations whose degree is proportional to the bandwidth $p+q+1$ of the matrix.

4.1. Boundary condition independent (Toeplitz) spectrum. The algorithm for the pure Toeplitz spectrum is based on the observation that separated the spectrum into two groups, i.e., we seek those eigensolutions whose κ's satisfy (3.1) with the equality (3.3). First we seek the solutions of the algebraic equation (2.6) with two distinct but equal modulus κ's. We denote these κ's by

(4.1) $$\kappa_a = \hat{\kappa} e^{i\psi_\ell}, \quad \kappa_b = \hat{\kappa} e^{-i\psi_\ell}, \quad 0 < \psi_\ell < \pi$$

where $\hat{\kappa}$ is a complex variable. For computational convenience, the interval $[0, \pi]$ is divided into $M+1$ subintervals of size $\Delta\psi$ where $(M+1)\Delta\psi = \pi$ and $\psi_\ell = \ell\Delta\psi$, $\ell = 1, 2, \cdots, M$. (The choice of the integer M determines the number of computed points on the spectrum, i.e., the resolution of the spectrum, but does not affect the accuracy of the computed points.) An equation for $\hat{\kappa}$ (independent of λ) is easily obtained. Since κ_a and κ_b must each give the same value of λ when inserted in (2.6), we can eliminate λ and obtain a polynomial in $\hat{\kappa}$ with coefficients which are functions of the Toeplitz matrix elements and ψ_ℓ. In particular,

(4.2) $$\lambda(\kappa_a) = \sum_{m=-p}^{q} a_m \hat{\kappa}^m e^{im\psi_\ell}, \qquad \lambda(\kappa_b) = \sum_{m=-p}^{q} a_m \hat{\kappa}^m e^{-im\psi_\ell}$$

and since

(4.3) $$\lambda(\kappa_a) = \lambda(\kappa_b)$$

one obtains a polynomial equation of order $p+q$ for $\hat{\kappa}$:

$$\sum_{m=-p}^{q} a_m \sin(m\psi_\ell)\hat{\kappa}^m = 0. \tag{4.4}$$

The algorithm for the boundary condition independent spectrum is:

Algorithm 4.1

For each of the M values of ψ_ℓ:

(i) Solve equation (4.4) for the $p+q$ roots $\hat{\kappa}$.

(ii) Check the corresponding κ's to determine if they satisfy (3.1) with (3.3), i.e., that κ_a and κ_b from (4.1) are in fact κ_p and κ_{p+1}. This is done as follows.

For each $\hat{\kappa}$ obtained in (i)

(iia) Calculate κ_a and κ_b from (4.1) and insert κ_a (or κ_b) in (2.6) to find λ. Substitute this value for λ back into (2.6) and solve the algebraic equation to determine the remaining $(p+q-2)$ κ's.

(iib) If the $p+q$ κ's satisfy the inequality (3.1) with (3.3), i.e., $|\kappa_a| = |\kappa_b| = |\kappa_p| = |\kappa_{p+1}|$, then λ is a point on the asymptotic Toeplitz spectrum. If the κ's do not satisfy the inequality test, discard the λ.

Return to (iia) until all $\hat{\kappa}$'s from (i) have been tested.

Replace ψ_ℓ by $\psi_{\ell+1}$ and return to step (i).

It should be emphasized that the algorithm (4.1) requires the solution of many algebraic equations but their degree is proportional to the bandwidth of the matrix and not the order of the matrix. Note that the boundary conditions do not enter the calculation. An implementation of the algorithm in MATLAB is given in the Appendix . The algorithm will become more transparent in the examples of Section 6.

4.2. Boundary condition dependent spectrum. The algorithm for the boundary condition dependent spectrum closely parallels the eigenvalue analysis of Kreiss [7] and Gustafsson, Kreiss, and Sundström [6]. There are however some differences since their analysis for hyperbolic initial-boundary-value problems makes two assumptions: (I) Cauchy stability (an assumption about the eigenvalues of the Toeplitz matrix's circulant cousin) and (II) the quarter-plane eigensolutions are *unstable* (i.e., the eigenvalues are in a particular part of the complex plane). Since we are interested in the entire spectrum for any quasi-Toeplitz matrix, we do not impose conditions (I) and (II). The relaxation of these two conditions leads to a slightly more complicated algorithm.

The algorithm for the boundary condition dependent part of the spectrum is straightforward. We seek p (or q) values of κ which satisfy (2.6) and satisfy the left p (or right q) boundary difference equations. The remaining q (or p) κ's must satisfy (3.1) with inequality (3.4). The algorithm for the eigenvalues associated with the *left* boundary is:

Algorithm 4.2

(i) Assume a solution of the form

$$\phi_j = \sum_{m=1}^{p} \beta_m \kappa_m^j. \tag{4.5}$$

Substitute ϕ_j from (4.5) into the p left boundary difference equations (2.11) to obtain p equations for the $2p+1$ unknowns: p κ_m's, p β_m's, and λ. These p equations are linear and homogeneous in the β's therefore the nontrivial solutions reduce the system to a single equation for the p κ's and λ. An additional p equations are required and they are derived from the algebraic equation (2.6) since each of the p κ's must give the same value of λ. This system of polynomial equations can be reduced to a single polynomial equation for a single variable and we choose κ_p.

(ii) The roots of the algebraic equation from (i) contain all *candidate* κ_p's for the (left) boundary condition dependent spectrum. For each κ_p the corresponding κ_m's must be checked. This is accomplished by calculating the corresponding λ ($\kappa = \kappa_p$) from (2.6) and then computing the $p+q$ roots of (2.6) for the given λ. Finally, we compare those roots with the p κ_m's which satisfy the boundary difference equations (2.11). If (3.1) and (3.4) are both satisfied, the λ is an eigenvalue in the boundary condition dependent part of the spectrum.

The algorithm for the eigenvalues associated with the right boundary is similar. If the algorithm has been implemented for the left boundary problem, it can be used for the right boundary problem by pre- and post-multiplying **A** by the permutation matrix

$$\mathbf{P} = \begin{bmatrix} & & & & 1 \\ & O & & 1 & \\ & & \cdot & & \\ & & \cdot & & \\ & 1 & & O & \\ 1 & & & & \end{bmatrix}, \tag{4.6}$$

i.e., **PAP**. Note that $\mathbf{P}^{-1} = \mathbf{P}$. The matrix **PAP** is most easily obtained by interchanging the columns of **A** "left to right" and then interchanging the rows "up and down". The boundary difference equations associated with the left boundary for **PAP** are

$$\mathbf{C}\tilde{\boldsymbol{\phi}} = \lambda \mathbf{D}\tilde{\boldsymbol{\phi}}. \tag{4.7}$$

As an example, the matrices **C** and **D** associated with **PAP** where **A** is (1.4) are

$$\mathbf{C} = \begin{bmatrix} c_{11} & c_{12} & c_{13} & c_{14} \\ c_{21} & c_{22} & c_{23} & c_{24} \end{bmatrix}, \quad \mathbf{D} = \begin{bmatrix} 1 & 0 & 0 & 0 \\ 0 & 1 & 0 & 0 \end{bmatrix}. \tag{4.8}$$

This explains the somewhat unconventional indexing for the c elements of (1.4). (Note that a pure Toeplitz matrix **A** is persymmetric, i.e., it is symmetric about its northeast-southwest diagonal [3]. Consequently $\mathbf{A}^T = \mathbf{PAP}$. However if **A** is *quasi*-Toeplitz then **PAP** is *not* the transpose of **A**.)

The details of the algorithm are illustrated by the examples of Section 6. Note that there *may* be no eigenvalues from the boundary condition dependent part of the spectrum even if non-Dirichlet boundary conditions are specified, i.e., the set of eigenvalues corresponding to group (b) defined by (3.4) may be empty.

The algorithm for the boundary condition dependent spectrum is straightforward but finding a polynomial equation in a single variable can be algebraically involved and the degree of the polynomial can be large. The system of equations for the κ's in (i) are symmetric polynomials therefore the algebraic complexity can be somewhat reduced by the use of the elementary symmetric functions. We have implemented algorithm 4.2 in MACSYMA and it performs satisfactorily on an IRIS workstation for the matrix **B** with two rows and a quasi-Toeplitz matrix **A** with bandwidths up to five.

4.3. Alternative boundary condition dependent algorithm. The algebraic complexity of the boundary condition dependent algorithm of Section 4.2 led us to consider alternative methods. In the GKS (Gustafsson, Kreiss and Sundström [6]) theory a GKS (i.e., *unstable*) eigenvalue is a member of the boundary condition dependent eigenvalue set of this paper. Kreiss [7] recognized that it is often very difficult to find GKS eigenvalues by analytical methods. He proposed finding GKS eigenvalues (if they exist) by a numerical eigenvalue computation of the finite-domain problem where the boundary condition (or conditions) to be checked are on the left boundary and Dirichlet boundary conditions are imposed on the right boundary. Kreiss showed that GKS eigenvalues converge exponentially fast with increasing J. We found however difficulties in numerically delineating the GKS eigenvalues (or other boundary condition dependent eigenvalues) for *non-normal* matrices. The numerical difficulties are often alleviated if the matrix is rescaled as described in Section 7.

We have found the following algorithm to be useful although not always completely reliable since it will sometimes "miss" an eigenvalue. The reliability is improved if the algorithm is repeated for several matrix orders.

Algorithm 4.3

(i) Place the boundary conditions of interest on the left boundary and Dirichlet conditions on the right boundary.

(ii) Apply the similarity transformation described in Section 7 and use a conventional eigenvalue algorithm to find the eigenvalues for large J.

(iii) Test all eigenvalues found in (ii) using Part (ii) of algorithm 4.2.

5. Numerical application of algorithms. Plots of the spectra of Toeplitz matrices present some interesting and sometimes surprising geometrical shapes. In this section we present some spectra which were obtained with the algorithms described in section 4. The matrix coefficients were selected more or less at random to give a flavor of the geometric patterns that may occur.

In each figure we show the spectra plotted in the complex plane. Open circles represent numerically computed eigenvalues for the matrix order (J) specified in the figure legend. The "solid" line (which is formed by closely spaced dots) is the asymptotic spectrum for the Toeplitz matrix and was computed using algorithm 4.1. The star symbol ($*$) is used to represent the boundary condition dependent part of the asymptotic spectrum computed using algorithm 4.2 or 4.3. The dashed line represents the spectrum for the circulant cousin of the pure Toeplitz matrix.

5.1. Toeplitz spectra. First we summarize the known properties of the asymptotic spectra of pure Toeplitz matrices and show some examples which illustrate these properties.

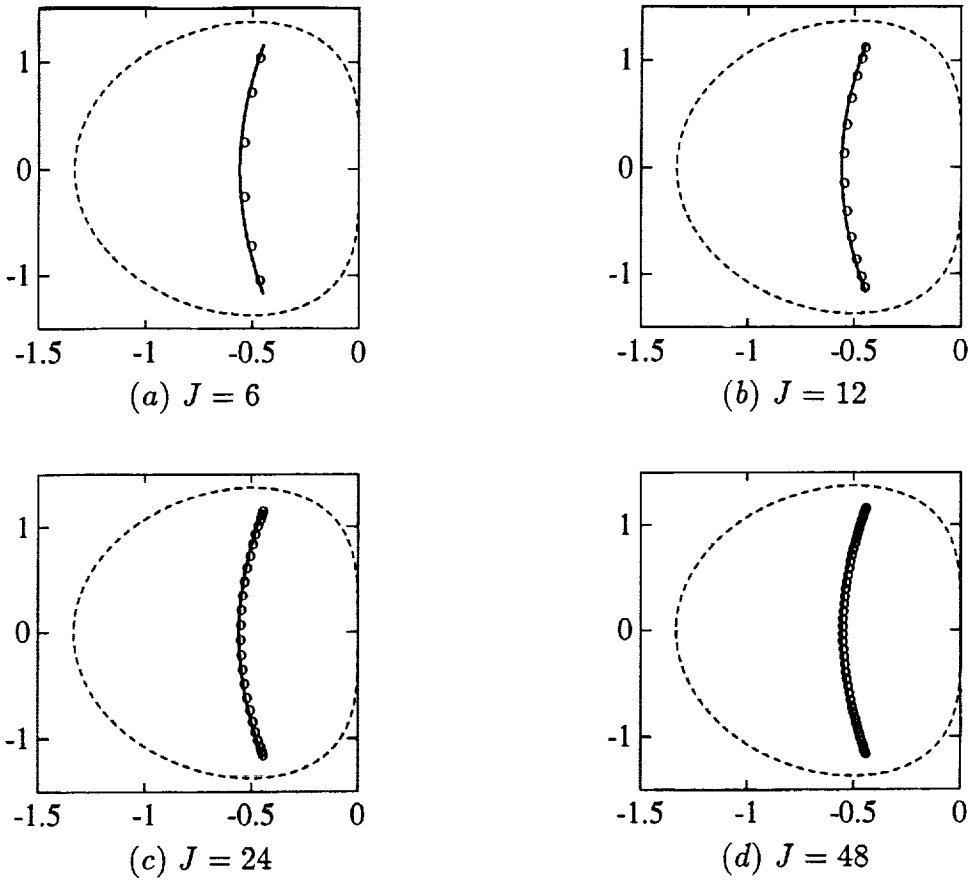

FIGURE 5.1. *Toeplitz matrix* $[-1/3, -1/2, 1, -1/6]$ *spectra "fill in" for increasing matrix order* J. *The symbol o denotes a numerically computed eigenvalue. Asymptotic spectra (algorithm 4.1) are denoted by "solid" lines and asymptotic circulant spectra (2.17) by dashed lines.*

Let $\mathbf{A}_J$ denote a $J \times J$ pure Toeplitz matrix where $\lambda(\mathbf{A}_J) = \{\lambda_1, \lambda_2, \cdots, \lambda_J\}$ denotes the spectrum. Consider a sequence of matrices $\mathbf{A}_J$ where the dimension J tends to infinity. As J increases a subset of the complex plane is "filled in" by the eigenvalues $\lambda(\mathbf{A}_J)$ as $J \rightarrow \infty$ and one obtains the asymptotic spectrum [9]. This is illustrated in Fig. 5.1 for a quadridiagonal pure Toeplitz matrix defined by the sequence (2.16). Note that the spectrum $\lambda(\mathbf{A}_J)$ is close to the asymptotic spectrum even for small values of J.

The asymptotic spectrum of a banded pure Toeplitz matrix is compact and locally it consists of analytical arcs [9]. Furthermore, it possesses no isolated points [13]. This property will be of interest in considering the asymptotic spectra of quasi-Toeplitz matrices. Ullman [13] has shown that the asymptotic spectrum is connected. Asymptotic spectra illustrating these properties are plotted in Figs. 5.2 and 5.3. The defining sequence (1.1) is shown under each figure. Algorithm 4.1 is not restricted to Toeplitz matrices with *real* coefficients and this is demonstrated in Fig. 5.3d. As the bandwidth of the matrix increases, the asymptotic spectrum becomes increasingly complex.

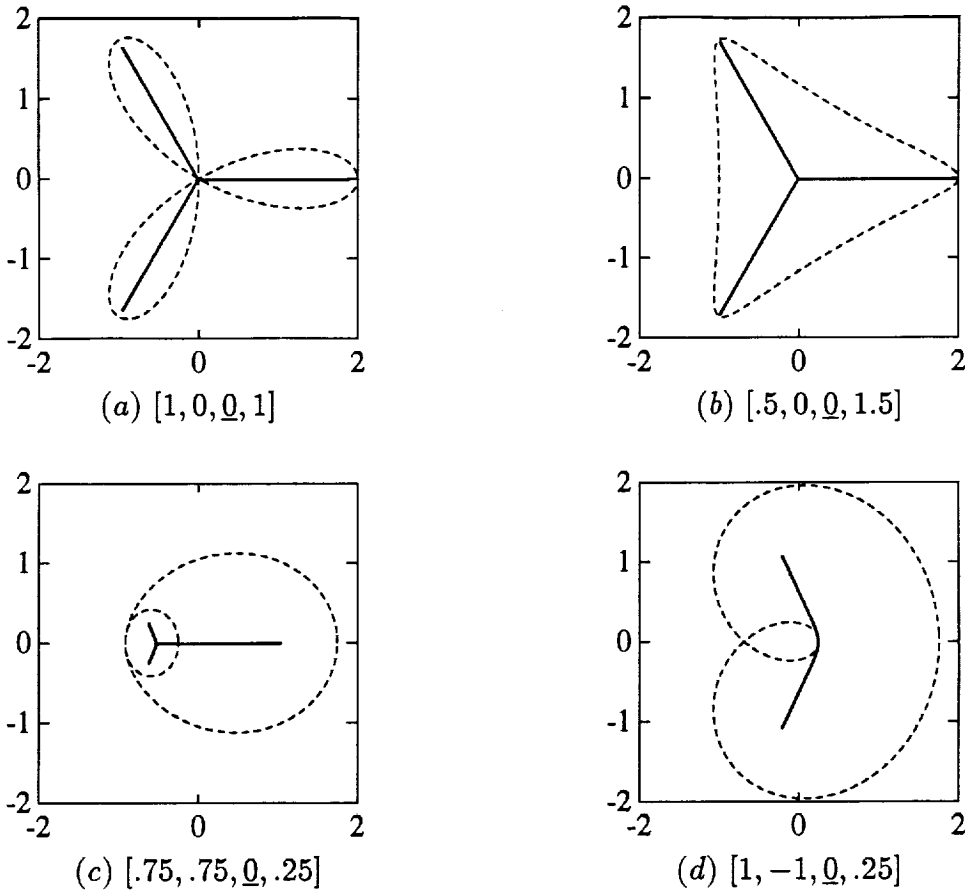

FIGURE 5.2. *Asymptotic spectra for pure Toeplitz matrices (algorithm 4.1) indicated by "solid" lines and the asymptotic spectra for the circulant cousin Toeplitz matrices indicated by dashed lines.*

According to Schmidt and Spitzer [9] it is not easy to give a simple geometric description of the asymptotic Toeplitz spectrum for non-normal matrices. An exception is the special case where the defining sequence is $[a_{-p}, 0, \cdots, 0, a_q]$, i.e., all members of the sequence are zero except the two "outriders". In this case the spectrum is a star-shaped figure. Examples of star-shaped spectra for quadridiagonal matrices are shown in Figs. 5.2a,b and for a septadiagonal matrix in Fig. 5.3a. The spectrum for the tridiagonal case is known analytically and consists of a straight line segment (connecting the foci of the ellipse which is the spectrum of its circulant cousin) [15].

It is a general result [9] that the asymptotic Toeplitz spectrum is "enclosed" by the spectrum of its circulant cousin. This is illustrated in Figs. 5.2 and 5.3. However, for finite J the spectrum $\lambda(\mathbf{A}_J)$ of $\mathbf{A}$ is not necessarily enclosed by the asymptotic spectrum of the circulant cousin of $\mathbf{A}$. This is illustrated in Fig. 5.4.

5.2. Quasi-Toeplitz spectra. The properties of the asymptotic spectrum of a quasi-Toeplitz matrix are illustrated in Fig. 5.5 for the matrix (1.7). The asymptotic spectrum consists of the asymptotic pure Toeplitz spectrum, group (a), plus (possible) isolated eigen-

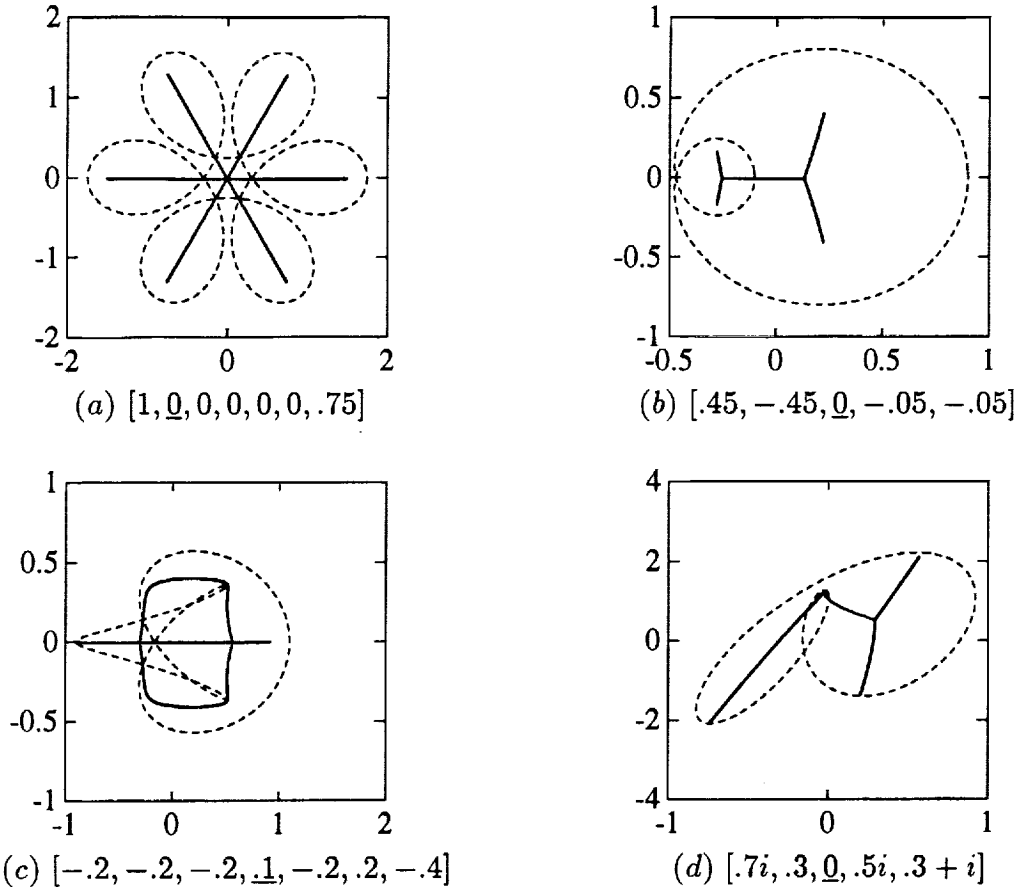

FIGURE 5.3. *Asymptotic spectra for Toeplitz matrices (algorithm 4.1) indicated by "solid" lines and their circulant cousin Toeplitz matrices indicated by dashed lines.*

values corresponding to boundary condition dependent eigenvalues, group (b). The isolated eigenvalues (see, e.g., Fig. 5.5b) must be boundary condition dependent eigenvalues associated with group (b) because the pure Toeplitz spectrum can have no isolated points [9]. Note also that, in contrast to the pure Toeplitz spectrum, the quasi-Toeplitz spectrum may have (isolated) eigenvalues outside the circulant spectrum, e.g., Figs. 5.5b,c,d. For $\alpha = \beta = 0$ the matrix (1.7) has no boundary condition dependent eigenvalues and the asymptotic quasi-Toeplitz spectrum is the pure Toeplitz spectrum shown in Fig. 5.5a. In this example group (b) is empty. A fundamental property of the eigenvalues associated with group (b) is that the "left" and "right" boundary dependent eigenvalues are uncoupled. This is illustrated in Fig. 5.5b,c,d. For $\beta = -.8$ there are three isolated eigenvalues to the right of the pure Toeplitz spectrum. These eigenvalues are completely independent of the parameter α of the left boundary condition (see matrix (1.7)). This fact is illustrated by comparing Figs. 5.5b,c where β is fixed and α is changed. For $\alpha = 1.2$ there is one isolated eigenvalue to the left of the circulant spectrum. This eigenvalue is independent of the parameter β of the right boundary condition as is indicated by comparing Figs. 5.5b,d.

6. Analytical application of algorithms. If the bandwidth of the matrix is suffi-

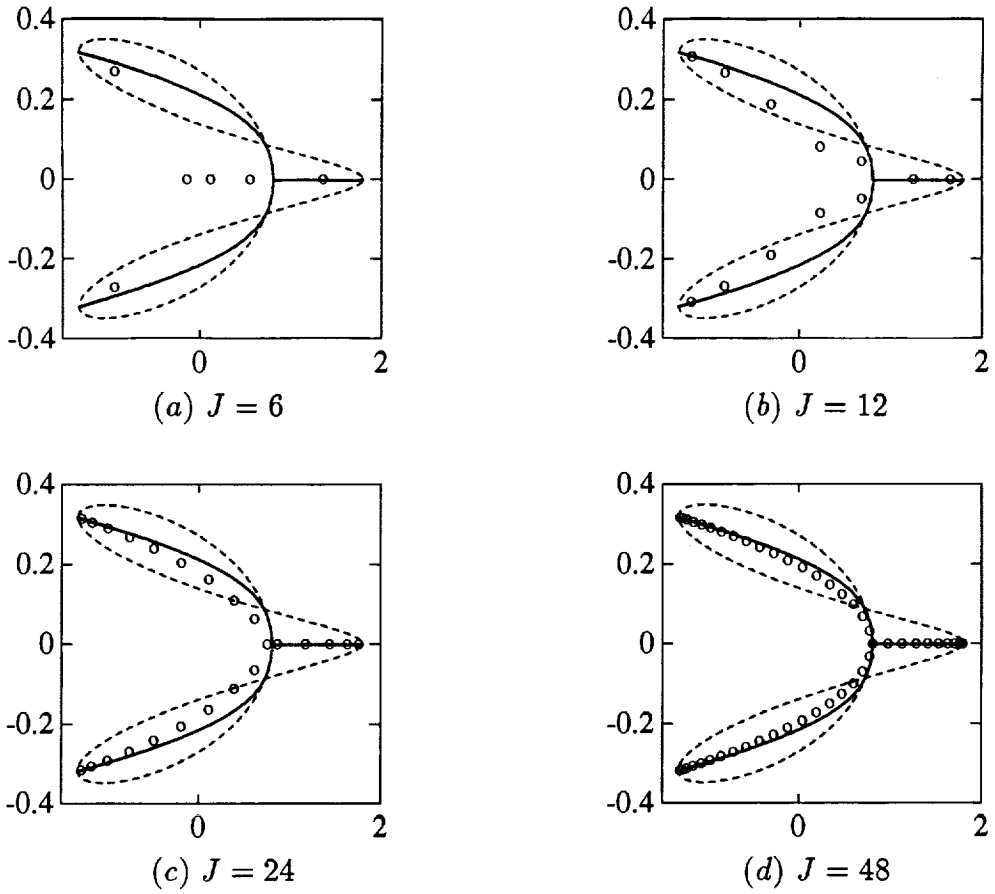

FIGURE 5.4. *Spectra for finite matrix order J (o symbol) and the asymptotic circulant spectrum (dashed lines). Asymptotic Toeplitz spectra indicated by "solid" lines. The Toeplitz matrix is* $[.7, .1, \underline{0}, .4, .6]$.

ciently small (≈ 3) the algorithms of Section 4 can be used as analytical methods. In this section we elucidate the algorithms of the previous section by considering small bandwidth examples for both Toeplitz and quasi-Toeplitz matrices.

6.1. Toeplitz tridiagonal matrix. A tridiagonal Toeplitz matrix is defined by the sequence $[a_{-1}, a_0, a_1]$ where $p = q = 1$ (see (1.1)). For this case the spectrum for arbitrary order J can be determined analytically. The solution is "well-known" although the eigenvalue formula does not appear in many references. A derivation is given by Smith [10, p. **]. The algebraic equation (2.6) becomes

$$\lambda = a_{-1}\kappa^{-1} + a_0 + a_1\kappa. \tag{6.1}$$

By rewriting (6.1), one obtains

$$a_1\kappa^2 + (a_0 - \lambda)\kappa + a_{-1} = 0. \tag{6.2}$$

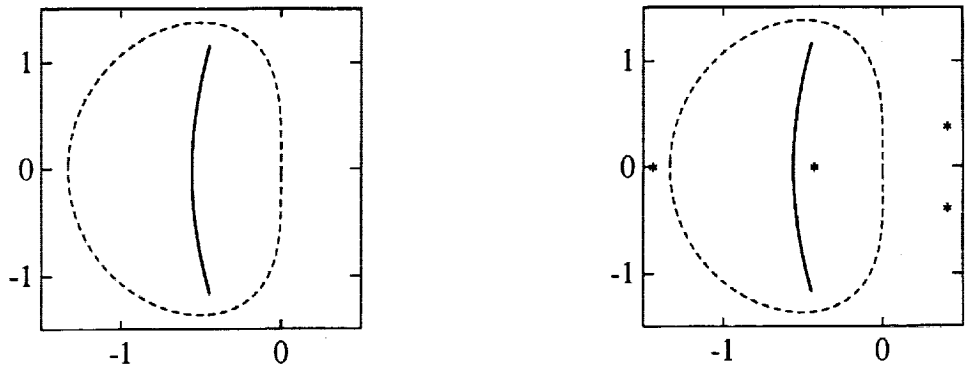

(a) $\alpha = 0,\ \beta = 0$ (b) $\alpha = 1.2,\ \beta = -.8$

(c) $\alpha = 0,\ \beta = -.8$ (d) $\alpha = 1.2,\ \beta = 0$

FIGURE 5.5. *Asymptotic spectra for the quasi-Toeplitz matrix (1.7). Boundary condition independent spectra computed with algorithm 4.1 ("solid" line) and boundary condition dependent spectra (∗ symbol) computed with algorithm 4.2.*

We denote the roots of this quadratic by κ_1, κ_2. The product of the roots is

$$\kappa_1 \kappa_2 = \frac{a_{-1}}{a_1}. \tag{6.3}$$

We follow the algorithm for the boundary condition independent part of the spectrum from Section 4.1. Equation (4.4) for $\hat{\kappa}$ reduces to

$$a_1 \hat{\kappa}^2 - a_{-1} = 0. \tag{6.4}$$

In step (i) we solve for the roots of (6.4), i.e.,

$$\hat{\kappa} = \pm\sqrt{a_{-1}/a_1}. \tag{6.5}$$

In step (iia) we find

$$\kappa_a = \sqrt{a_{-1}/a_1}\, e^{i\psi_\ell}, \quad \kappa_b = \sqrt{a_{-1}/a_1}\, e^{-i\psi_\ell} \tag{6.6a,b}$$

where we have chosen the positive square root. (The negative square root gives the same spectrum.) Since there are only two roots of (6.1), i.e., κ_1 and κ_2, they must be κ_a and κ_b. They obviously have equal modulus, therefore equality (3.3) is satisfied and the corresponding λ is part of the Toeplitz spectrum. (In this simple example step (ii) of the algorithm 4.1 is rather trivial.) Substitution of κ_a given by (6.6a) into (6.1) yields

$$\lambda_\ell = a_0 + 2\sqrt{a_1 a_{-1}}\cos\psi_\ell, \quad 0 < \psi_\ell < \pi \tag{6.7}$$

which is the asymptotic spectrum for a tridiagonal Toeplitz matrix.

Although not part of the asymptotic analysis we note that for the tridiagonal case, the roots κ_1 and κ_2 have equal modulus regardless of the order J of the matrix. In fact, the exact roots are given by

$$\kappa_1 = \hat{\kappa}e^{i\psi_\ell}, \qquad \kappa_2 = \hat{\kappa}e^{-i\psi_\ell}, \quad \text{where} \quad \psi_\ell = \ell\pi/(J+1), \quad \ell = 1, 2, \cdots, J \tag{6.8}$$

and $\hat{\kappa}$ is given by (6.5) (see, e.g. [15]). Consequently, the exact spectrum for a $J \times J$ matrix is (6.7) where ψ_ℓ is defined in (6.8). It should be emphasized that if the bandwidth of a Toeplitz matrix is larger than three, then algorithm 4.1 is, in general, exact only in the asymptotic limit $J \to \infty$.

6.2. Quasi-Toeplitz tridiagonal matrix. The asymptotic spectrum for a quasi-Toeplitz tridiagonal matrix is given by (6.7) plus any boundary condition dependent eigenvalues. We first show that a pure Toeplitz tridiagonal matrix does not have any boundary condition dependent eigenvalues, i.e., the homogeneous (Dirichlet) boundary conditions (2.4) introduce no boundary condition dependent eigenvalues. For a tridiagonal matrix the homogeneous conditions (2.4) are simply

$$\phi_0 = 0, \quad \phi_{J+1} = 0. \tag{6.9a,b}$$

By substituting (4.5), i.e.,

$$\phi_j = \beta_1 \kappa_1^j \tag{6.10}$$

into (6.9a), one concludes that either $\beta_1 = 0$ or $\kappa_1 = 0$. Since the product of the roots (6.3) is nonzero, then $\beta_1 = 0$ and there is no nontrivial eigenfunction and no eigenvalue is introduced by the (left) boundary condition (6.9a). By substituting (6.10) into (6.9b), one finds the similar result that no eigenvalue is introduced by the (right) boundary condition (6.9b).

For the general Toeplitz matrix there are p homogeneous Dirichlet boundary conditions at the left boundary and q homogeneous Dirichlet boundary conditions at the right boundary, i.e., (2.4a,b). Substitution of (4.5) into the left boundary conditions leads to a homogeneous system $\mathbf{V}\boldsymbol{\beta} = 0$ where $\mathbf{V}$ is a $p \times p$ Vandermonde matrix and $\boldsymbol{\beta} = [\beta_1, \beta_2, \cdots, \beta_p]^T$. The determinant of $\mathbf{V}$ equals zero iff two κ's are equal which violates the assumption of distinct κ's. Therefore Dirichlet boundary conditions introduce no boundary condition dependent eigenvalues.

Consider now boundary conditions that introduce nontrivial solutions. Suppose that when (6.10) is introduced into the left boundary condition we obtain

$$\kappa_1 = \kappa_\sigma \tag{6.11}$$

where κ_σ is some nonzero complex constant. Does this introduce an eigenvalue? It does if inequality (3.4) is satisfied, i.e., $|\kappa_1| < |\kappa_2|$. From (6.3) one obtains

$$|\kappa_2| = |a_{-1}/a_1|/|\kappa_\sigma|. \tag{6.12}$$

Inequality (3.4) is satisfied if

$$|\kappa_1| = |\kappa_\sigma| < \sqrt{|a_{-1}/a_1|} \tag{6.13}$$

and the corresponding eigenvalue λ is obtained by substituting κ_σ into (6.1).

We give an example of a quasi-Toeplitz matrix where there is a boundary condition dependent eigenvalue. Consider the matrix

$$\mathbf{A} = \begin{bmatrix} 0 & -2 & 2 & & & & \\ -1 & 0 & 1 & & & O & \\ & \cdot & \cdot & \cdot & & & \\ & & \cdot & \cdot & \cdot & & \\ & & & \cdot & \cdot & \cdot & \\ & O & & & -1 & 0 & 1 \\ & & & & & -1 & 0 \end{bmatrix}. \tag{6.14}$$

Here

$$a_{-1} = -1, \quad a_0 = 0, \quad a_1 = 1, \quad b_{11} = 0, \quad b_{12} = -2, \quad b_{13} = 2. \tag{6.15}$$

The eigenvalue problem is (2.3) with $p = q = 1$ and the boundary difference equation (2.11) is

$$-2\phi_2 + 2\phi_3 = \lambda\phi_1. \tag{6.16}$$

Substitution of (6.10) into (6.16) yields

$$-2\kappa_1 + 2\kappa_1^2 = \lambda. \tag{6.17}$$

The second equation relating κ_1 and λ is (6.2) with $\kappa = \kappa_1$ and coefficients (6.15):

$$\kappa_1^2 - \lambda\kappa_1 - 1 = 0. \tag{6.18}$$

Elimination of λ from (6.17) and (6.18) yields

$$(\kappa_1 - 1)^2(2\kappa_1 + 1) = 0. \tag{6.19}$$

The roots of (6.19) are

$$\kappa_1 = 1, 1, -1/2. \tag{6.20}$$

In the tridiagonal case, step (ii) of algorithm 4.2 is simplified to checking inequality (6.13). The inequality (6.13), with (6.15),

$$|\kappa_1| = |\kappa_\sigma| < 1$$

is satisfied for $\kappa_1 = -1/2$. Substitution of $\kappa_1 = -1/2$ into (6.17) gives $\lambda = 3/2$.

The asymptotic spectrum of the quasi-Toeplitz matrix (6.14) consists of two parts. The boundary condition independent (pure Toeplitz) spectrum is (6.7):

$$\lambda = i2\cos\psi, \quad 0 < \psi < \pi \tag{6.21}$$

and the boundary condition dependent part of the spectrum is $\lambda = 3/2$. Consequently, the asymptotic spectrum is a line segment on the imaginary axis between $\pm 2i$ and the single eigenvalue $\lambda = 3/2$.

6.3. Toeplitz quadridiagonal matrix. A more interesting example is the quadridiagonal matrix (1.3) where $p = 1$ and $q = 2$. The algebraic equation (2.6) is

$$\lambda = a_{-1}\kappa^{-1} + a_0 + a_1\kappa + a_2\kappa^2. \tag{6.22}$$

For the boundary condition independent spectrum, the three roots of the cubic (6.22) must satisfy (3.1) and (3.3)

$$|\kappa_1| = |\kappa_2| \le |\kappa_3|. \tag{6.23}$$

The product of the roots of (6.22) is $-a_{-1}/a_2$ and therefore

$$|\kappa_1||\kappa_2||\kappa_3| = |a_{-1}/a_2|. \tag{6.24}$$

The polynomial (4.4) for $\hat{\kappa}$ becomes

$$a_{-1}\sin(-\psi_\ell)\hat{\kappa}^{-1} + a_1\sin(\psi_\ell)\hat{\kappa} + a_2\sin(2\psi_\ell)\hat{\kappa}^2 = 0$$

or

$$2a_2(\cos\psi_\ell)\hat{\kappa}^3 + a_1\hat{\kappa}^2 - a_{-1} = 0. \tag{6.25}$$

In (i) of algorithm 4.1 we solve (6.25) numerically for specified coefficients a_ℓ.

In (iia) of the algorithm 4.1 we proceed as follows. For each root $\hat{\kappa}$ we substitute $\kappa_a = \hat{\kappa}e^{i\psi_\ell}$ into (6.22) and calculate the corresponding λ. Then with λ given, we solve the cubic (6.22) for the roots $\kappa_1, \kappa_2, \kappa_3$. Of course, two of the roots are already known, i.e.,

$\kappa_a = \hat{\kappa}e^{i\psi_\ell}$ and $\kappa_b = \hat{\kappa}e^{-i\psi_\ell}$. In (iib) we check to see if the three roots satisfy inequality (6.23):

$$|\kappa_a| = |\kappa_b| = |\kappa_1| = |\kappa_2| \leq |\kappa_3|. \tag{6.26}$$

If this inequality is satisfied, then the corresponding λ is a point of the boundary condition independent spectrum. If the κ's fail to satisfy inequality (6.26), we discard the λ. We repeat (i) and (ii) for all of the ψ_ℓ's where $\ell = 1, 2, \cdots, M$.

For the particular example under consideration, the test (6.26) can be simplified as follows. Recall that the roots of equal modulus κ_1 and κ_2 are denoted by (4.1) and rewrite (6.23) as

$$|\hat{\kappa}| = |\hat{\kappa}| \leq |\kappa_3| \tag{6.27}$$

and (6.24) as

$$|\hat{\kappa}||\hat{\kappa}||\kappa_3| = |a_{-1}/a_2|. \tag{6.28}$$

Inequality (6.27) is satisfied if

$$|\hat{\kappa}| \leq |a_{-1}/a_2|^{1/3}. \tag{6.29}$$

Hence if $|\hat{\kappa}|$ satisfies (6.29), then the corresponding λ computed by inserting $\kappa_a = \hat{\kappa}e^{i\psi_\ell}$ into (6.22) is a point of the boundary condition independent spectrum.

The spectrum for the Toeplitz matrix (1.3) with coefficients (2.16) was computed with algorithm 4.1 (see also the Appendix) and is the "solid" line in each of the figures of Fig. 5.1. The spectrum for the circulant cousin (1.6) is the dashed line in each of the figures of Fig. 5.1 (see (2.17)).

6.4. Quasi-Toeplitz quadridiagonal matrix. An example of a quasi-Toeplitz quadridiagonal matrix is (1.4) where $p = 1$ and $q = 2$. The eigenvalue problem is equivalent to (2.3), i.e.,

$$\lambda\phi_j = a_{-1}\phi_{j-1} + a_0\phi_j + a_1\phi_{j+1} + a_2\phi_{j+2}, \qquad j = 2, 3, \cdots, J \tag{6.30}$$

with left boundary difference equation (2.11):

$$b_{11}\phi_1 + b_{12}\phi_2 + b_{13}\phi_3 + b_{14}\phi_4 = \lambda\phi_1. \tag{6.31}$$

The spectrum for the matrix (1.4) is the spectrum for the pure Toeplitz matrix (plotted in Fig. 5.5b for coefficients (2.16)) plus any boundary condition dependent eigenvalues. For the boundary condition dependent spectrum the roots of the cubic (6.22) must satisfy

$$|\kappa_1| < |\kappa_2| \leq |\kappa_3| \tag{6.32}$$

(see (3.1) and (3.4)).

In the analysis of the boundary condition dependent part of the spectrum, the left and right boundary conditions are uncoupled and consequently we consider each boundary separately.

6.4.1. Left boundary dependent spectrum. The left boundary difference equation is given by (6.31). We follow the algorithm for the boundary condition dependent part of the spectrum given in Section 4.2. Recall that for this example $p = 1$ and in the first step (i) we look for a solution of the form (4.5)

$$\phi_j = \beta_1 \kappa_1^j. \tag{6.33}$$

Insertion of this equation into the boundary difference equation (6.31) yields

$$b_{11} + b_{12}\kappa_1 + b_{13}\kappa_1^2 + b_{14}\kappa_1^3 = \lambda. \tag{6.34}$$

As a particular example we consider the special case for the matrix (1.4) where the coefficients a_ℓ are given by (2.16) and the coefficients b_{1j} are given by

$$b_{11} = -\alpha - 3/2, \quad b_{12} = 3\alpha + 2, \quad b_{13} = -3\alpha - 1/2, \quad b_{14} = \alpha. \tag{6.35}$$

The algebraic equation (6.22) with $\kappa = \kappa_1$ becomes

$$6\lambda = -\frac{2}{\kappa_1} - 3 + 6\kappa_1 - \kappa_1^2 = -(\kappa_1 - 1)(\kappa_1^2 - 5\kappa_1 - 2)/\kappa_1 \tag{6.36}$$

and the boundary difference equation (6.34) with coefficients (6.35) becomes

$$-(\alpha + 3/2) + (3\alpha + 2)\kappa_1 - (3\alpha + 1/2)\kappa_1^2 + \alpha\kappa_1^3 = \lambda. \tag{6.37}$$

If we eliminate λ from (6.36) and (6.37), the polynomial for κ_1 is

$$(\kappa_1 - 1)^3(3\alpha\kappa_1 - 1) = 0. \tag{6.38}$$

Note that if we formulate the problem in terms of the extrapolation boundary conditions (2.9), then (6.38) follows by inserting (6.33) into (2.9a).

Example 6.1. As our first example we let $\alpha = 0$ and (6.38) becomes

$$(\kappa_1 - 1)^3 = 0. \tag{6.39}$$

The repeated roots of (6.39) are

$$\kappa_1 = 1 \tag{6.40}$$

and from (6.36) the corresponding eigenvalue is $\lambda = 0$. Recall that the roots of the cubic equation (6.36) are denoted by κ_1, κ_2, and κ_2. By inserting $\lambda = 0$ into (6.36), one finds that the roots are

$$\kappa_1 = 1, \qquad \kappa_2 = (5 - \sqrt{33})/2 \approx -0.372, \qquad \kappa_3 = (5 + \sqrt{33})/2 \approx 5.372. \tag{6.41a,b,c}$$

It is obvious that inequality (6.32) is not satisfied. Therefore, if $\alpha = 0$ the left boundary condition does not introduce any boundary condition dependent eigenvalues.

Example 6.2. Although the boundary condition (6.34) with (6.35) and $\alpha = 0$ does not introduce any boundary condition dependent eigenvalues, they are introduced for a range of nonzero values of the parameter α. The roots of (6.38) are

$$\kappa_1 = 1,\ 1,\ 1,\ 1/(3\alpha) \qquad (\alpha \neq 0). \tag{6.42}$$

Are there any values of α for which $\lambda = 0$ is a boundary condition dependent eigenvalue? For $\lambda = 0$, the roots of (6.36) are

$$\kappa = 1, \quad \kappa = (5 - \sqrt{33})/2 \approx -0.372, \quad \kappa = (5 + \sqrt{33})/2 \approx 5.372. \tag{6.43}$$

It is obvious that inequality (6.32) is not satisfied if $\kappa_1 = 1$ which excludes the repeated roots in (6.42). Inequality (6.32) is satisfied if

$$\kappa_1 = (5 - \sqrt{33})/2 \approx -0.372, \quad \kappa_2 = 1, \quad \kappa_3 = (5 + \sqrt{33})/2 \approx 5.372. \tag{6.44a,b,c}$$

In order to have a boundary condition dependent eigenvalue $\lambda = 0$ we must choose α in (6.42), i.e.,

$$\kappa_1 = 1/(3\alpha) \tag{6.45}$$

so that κ_1 is (6.44a). By equating (6.45) and (6.44a), one obtains

$$\alpha = -(5 + \sqrt{33})/12 \approx -0.895. \tag{6.46}$$

Consequently, for this value of α the boundary condition (6.34) with (6.35) will introduce the boundary condition dependent eigenvalue $\lambda = 0$.

If one carries out a GKS normal mode analysis for the semi-discrete approximation with (2.16) and the numerical boundary condition (6.34) with (6.35), one finds that the semi-discrete approximation is unstable for $\alpha < \hat{\alpha}$ where $\hat{\alpha}$ is defined by (6.46).

As explicit formula for λ in terms of the parameter α is found by substituting (6.45) into (6.37):

$$\lambda = (3\alpha - 1)(-18\alpha^2 - 15\alpha + 1)/(54\alpha^2). \tag{6.47}$$

If one chooses a particular value of α, the corresponding value of λ is a boundary condition dependent eigenvalue if and only if the corresponding κ's satisfy inequality (6.32).

Example 6.3. Is it possible to choose α so that there is an eigenvalue

$$\lambda = -4/3 \tag{6.48}$$

which falls on the oval shaped circulant spectrum where the *oval* crosses the real axis (see Fig. 5.5a)? This value of λ is an eigenvalue of the circulant matrix (1.6) with (2.16) as one can easily verify from the formula (2.17) for $\theta = \pi$. (The corresponding κ for the circulant

case is $\kappa = -1$.) By substituting $\lambda = -4/3$ into the cubic equation (6.36) one obtains the roots

(6.49a,b,c) $\qquad \kappa = -1, \qquad \kappa = (7 - \sqrt{41})/2 \approx .298, \qquad \kappa = (7 + \sqrt{41})/2 \approx 6.70.$

Inequality (6.32) is satisfied if and only if

(6.50a,b,c) $\qquad \kappa_1 = (7 - \sqrt{41})/2 \approx .298, \qquad \kappa_2 = -1, \qquad \kappa_3 = (7 + \sqrt{41})/2 \approx 6.70$

If α in (6.45) is chosen so that κ_1 is (6.50a), one obtains

$$\alpha = 1/(3\kappa_1) = (7 + \sqrt{41})/12 \approx 1.117. \tag{6.51}$$

Hence $\lambda = -4/3$ is a point of the boundary condition dependent spectrum for the value of α given by (6.51).

6.4.2. Right boundary dependent spectrum. In the analysis for the boundary condition dependent part of the spectrum, the left and right boundary conditions are uncoupled. It is convenient to have a single algorithm for both the left and right boundary condition problems. This can be done by *switching* the matrix so that the right and left boundary conditions are interchanged. For example, if the matrix (1.4) is switched as described in Section 4.2 one obtains the the matrix:

$$\widehat{\mathbf{A}} = \begin{bmatrix} c_{11} & c_{12} & c_{13} & c_{14} & & & & \\ c_{21} & c_{22} & c_{23} & c_{24} & & & & \\ \hat{a}_{-2} & \hat{a}_{-1} & \hat{a}_0 & \hat{a}_1 & & & O & \\ & \cdot & \cdot & \cdot & \cdot & & & \\ & & \cdot & \cdot & \cdot & \cdot & & \\ & & & \cdot & \cdot & \cdot & \cdot & \\ & & O & & \hat{a}_{-2} & \hat{a}_{-1} & \hat{a}_0 & \hat{a}_1 \\ & & & & & \hat{a}_{-2} & \hat{a}_{-1} & \hat{a}_0 & \hat{a}_1 \\ & & & & & b_{14} & b_{13} & b_{12} & b_{11} \end{bmatrix} \tag{6.52}$$

where $\hat{a}_j = a_{-j}$. For this matrix $p = 2$ and $q = 1$ and the left boundary difference equations are given by

$$c_{11}\phi_1 + c_{12}\phi_2 + c_{13}\phi_3 + c_{14}\phi_4 = \lambda\phi_1 \tag{6.53a}$$

$$c_{21}\phi_1 + c_{22}\phi_2 + c_{23}\phi_3 + c_{24}\phi_4 = \lambda\phi_2. \tag{6.53b}$$

For the matrix (6.52), the algebraic equation (2.6) is

$$\lambda = \hat{a}_{-2}\kappa^{-2} + \hat{a}_{-1}\kappa^{-1} + \hat{a}_0 + \hat{a}_1\kappa. \tag{6.54}$$

There are two boundary conditions (6.53) and following the algorithm for the boundary condition dependent spectrum we seek a solution of the form (4.5), i.e.,

$$\phi_j = \beta_1\kappa_1^j + \beta_2\kappa_2^j. \tag{6.55}$$

From (6.53a,b) one obtains

(6.56a)

$$c_{11}(\beta_1\kappa_1+\beta_2\kappa_2)+c_{12}(\beta_1\kappa_1^2+\beta_2\kappa_2^2)+c_{13}(\beta_1\kappa_1^3+\beta_2\kappa_2^3)+c_{14}(\beta_1\kappa_1^4+\beta_2\kappa_2^4)=\lambda(\beta_1\kappa_1+\beta_2\kappa_2)$$

(6.56b)

$$c_{21}(\beta_1\kappa_1+\beta_2\kappa_2)+c_{22}(\beta_1\kappa_1^2+\beta_2\kappa_2^2)+c_{23}(\beta_1\kappa_1^3+\beta_2\kappa_2^3)+c_{24}(\beta_1\kappa_1^4+\beta_2\kappa_2^4)=\lambda(\beta_1\kappa_1^2+\beta_2\kappa_2^2).$$

Since κ_1 and κ_2 must each give the same λ, we use (6.54) to obtain two additional equations

$$\lambda=\hat{a}_{-2}\kappa_1^{-2}+\hat{a}_{-1}\kappa_1^{-1}+\hat{a}_0+\hat{a}_1\kappa_1 \tag{6.56c}$$

$$\lambda=\hat{a}_{-2}\kappa_2^{-2}+\hat{a}_{-1}\kappa_2^{-1}+\hat{a}_0+\hat{a}_1\kappa_2. \tag{6.56d}$$

The system of (four) equations (6.56) has (five) unknowns $\beta_1,\beta_2,\kappa_1,\kappa_2,\lambda$. Since the equations (6.56a,b) are linear and homogeneous in β_1 and β_2 and (6.56) are algebraic equations, they can be reduced to a single algebraic equation in a single variable (we choose κ_2), i.e.,

$$P(\kappa_2)=0. \tag{6.57}$$

The roots of (6.57) are all possible values of κ_2 which may introduce boundary condition dependent eigenvalues. Each κ_2 is tested as follows: Substitute $\kappa=\kappa_2$ into (6.54). Solve the new equation for $\lambda(\kappa_2)$. Substitute $\lambda(\kappa_2)$ back into (6.54) and solve the resulting equation for $\kappa_1,\kappa_2,\kappa_3$. If the κ's satisfy (3.1) with (3.4), i.e.,

$$|\kappa_1|\le|\kappa_2|<|\kappa_3| \tag{6.58}$$

then $\lambda(\kappa_2)$ is a boundary condition dependent eigenvalue, otherwise it is not part of the asymptotic spectrum.

If the bandwidth of the matrix is large and the number of rows in the boundary condition matrix **B** becomes large, the algebraic reduction of the system, e.g., (6.57), becomes hopeless even for good symbolic systems such as MACSYMA. In these cases we recommend the less reliable but more efficient algorithm of Section 4.3.

An alternative solution procedure for (6.56) is the following. The system of equations, e.g., (6.56) is symmetric in the κ's so the algebra can be simplified by the introduction of the elementary symmetric functions. As an example we consider the relatively simple right boundary problem for the matrix (1.7) and introduce the elementary symmetric functions [11]

$$y=\kappa_1+\kappa_2 \tag{6.59}$$

and

$$x=\kappa_1\kappa_2. \tag{6.60}$$

It can be shown that the system (6.56) reduces to

(6.61)
$$-c_{13}(\frac{\hat{a}_1}{\hat{a}_{-2}})^2 x^5 + \frac{2c_{13}\hat{a}_{-1}\hat{a}_1}{\hat{a}_{-2}^2}x^4 + [-\frac{c_{13}\hat{a}_{-1}^2}{\hat{a}_{-2}^2} + \frac{(\hat{a}_1 - c_{12})\hat{a}_1}{\hat{a}_{-2}}]x^3$$
$$+ [c_{13} - \frac{(\hat{a}_1 - c_{12})\hat{a}_{-1}}{\hat{a}_{-2}}]x^2 + (\hat{a}_0 - c_{11})x - \hat{a}_{-2} = 0$$

where $c_{11} = -3\beta$, $c_{12} = 3\beta - 1/2$, and $c_{13} = -\beta$ and

(6.62)
$$y = (\hat{a}_1 x^2 - \hat{a}_{-1}x)/\hat{a}_{-2}.$$

It is not practical to proceed analytically so for a particular set of matrix coefficients we solve (6.61) numerically for x and proceed as in the general algorithm 4.2.

7. Eigenvector scaling. If conventional numerical eigenvalue packages, e.g., IMSL, EISPACK, etc., are used to compute the spectra for non-normal Toeplitz matrices, large errors in the spectra may be encountered for matrices of relatively low order. For example if we choose the matrix

(7.1)
$$[-1/6, 1, \underline{-1/2}, -1/3]$$

and use the MATLAB routine $eig(\mathbf{A})$ on an IRIS workstation to compute the eigenvalues, we obtain the sequence of spectra (for increasing matrix order) shown in Figs. 7.1a through 7.1d. The Toeplitz matrix defined by (7.1) is the transpose of the Toeplitz matrix defined by (2.16).

If one computes the numerical spectra of the Toeplitz matrix (2.16), e.g., see Fig. 5.1, for $J = 80$ and 160, they would fall on the asymptotic spectra. In general, if one computes the numerical spectra of a nonnormal matrix $\mathbf{A}$ and its transpose $\mathbf{A}^T$ (for sufficiently large J) they will differ in spite of the fact that the analytical spectra are identical. This phenomenon is discussed at the end of this section.

A non-normal Toeplitz matrix (e.g., (7.1)) can have the property that the spectrum is very sensitive to perturbations of the matrix elements. For such matrices, Trefethen [12] and Reichel and Trefethen [8] suggest that an eigenvalue analysis may lead to incorrect conclusions and it is more meaningful to analyze *pseudo*-eigenvalues. The *erroneous* eigenvalues plotted in Fig. 7.1 are a manifestation of the pseudo-spectra of the matrix (7.1) for increasing J. The numerical error can be reduced by using higher numerical precision. However, for any numerical precision the qualitative behavior illustrated in Fig. 7.1 will always appear for sufficiently large J. Qualitatively, the numerical Toeplitz spectrum approaches the spectrum of its Toeplitz circulant cousin as $J \to \infty$.

The difficulty in numerically computing the eigenvalues of a non-normal Toeplitz matrix is related to the exponential character of the eigenvectors. We illustrate this with an example by comparing the eigenvectors of the matrix (2.16) with the eigenvectors of its transpose (7.1). Since (2.16) is a Toeplitz matrix, the asymptotic spectrum is independent of the boundary conditions and the κ roots satisfy (6.23). In this example the moduli

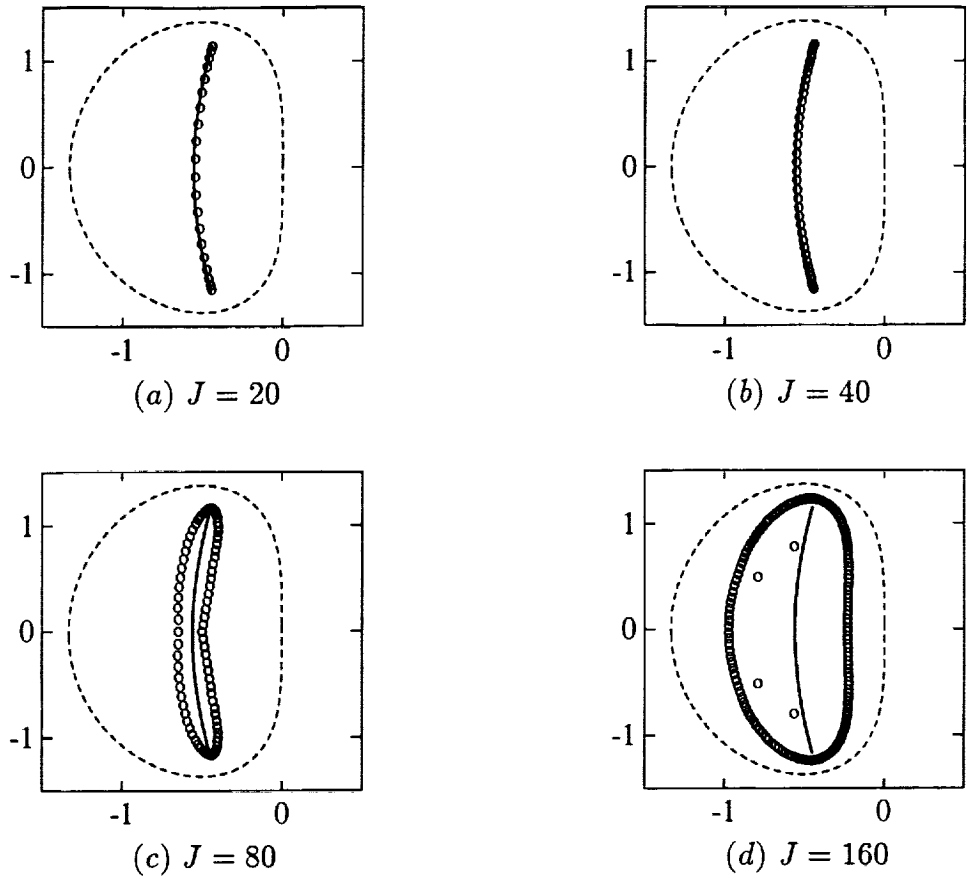

FIGURE 7.1. *Numerically computed spectra (o symbol) for the unscaled Toeplitz matrix* $[-1/6, 1, -1/2, -1/3]$. *Asymptotic Toeplitz spectra and asymptotic circulant spectra indicated by "solid" and dashed lines, respectively.*

of the roots of equal modulus (4.1), $|\hat{\kappa}|$, are only weakly dependent on the angle ψ_ℓ as illustrated in Fig. 7.2. From (4.4) with coefficients given by (2.16) and $\psi = \pi/2$ one obtains $|\hat{\kappa}| = 1/\sqrt{3}$. Hence for the roots of equal modulus, one finds

$$|\kappa_1| = |\kappa_2| = |\hat{\kappa}| \approx 1/\sqrt{3} \tag{7.2}$$

and consequently the moduli of the eigenvector elements behave as

$$|\phi_j| \approx (1/\sqrt{3})^j \tag{7.3}$$

i.e., they exponentially decrease with increasing j.

For the transpose $\mathbf{A}^T$, defined by (7.1), one has

$$|\check{\kappa}_1| \leq |\check{\kappa}_2| = |\check{\kappa}_3| \tag{7.4}$$

where the check symbol indicates that the κ's in (6.23) and (7.4) are not the same. In fact, the κ's of (6.23) and (7.4) are reciprocals. Consequently, for $\mathbf{A}^T$ one has

$$|\check{\kappa}_2| = |\check{\kappa}_3| = |\hat{\kappa}| \approx \sqrt{3} \tag{7.5}$$

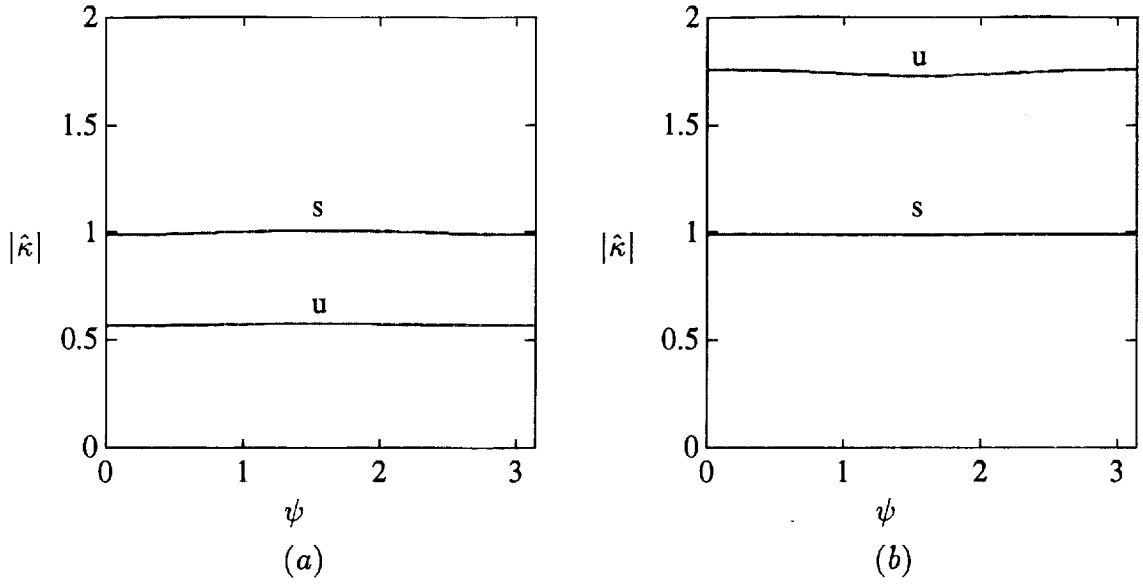

FIGURE 7.2. *Modulus of $\hat{\kappa}$ vs ψ_ℓ for (a) matrix (2.16) unscaled, u, and scaled, s, and (b) the transpose matrix (7.1) unscaled, u, and scaled, s.*

and the moduli of the eigenvector elements

$$|\phi_j| \approx (\sqrt{3})^j \tag{7.6}$$

grow exponentially with increasing j.

A simple scaling attenuates the exponential behavior of the eigenvectors. Let $\mathbf{A}$ denote an arbitrary banded Toeplitz matrix. If the κ's of equal modulus (3.3) are not on the unit circle, then either $\mathbf{A}$ or $\mathbf{A}^T$ will have exponentially growing eigenvectors. Assume that $\mathbf{A}$ has κ's of equal modulus (4.1) which are outside the unit circle. Define $\tilde{\kappa}$ to be

$$\tilde{\kappa} = \underset{0<\psi_\ell<\pi}{\text{mean}}(|\hat{\kappa}|). \tag{7.7}$$

For the matrix $\mathbf{A}$ we rescale the eigenvectors by

$$\tilde{\phi}_j = \frac{\phi_j}{\tilde{\kappa}^j}. \tag{7.8}$$

The scaling is effectively a normalization of the $\hat{\kappa}$'s so their moduli are approximately equal to unity.

The *scaling* similarity transformation is

$$\mathbf{S}^{-1} = \begin{bmatrix} 1/\tilde{\kappa} & & & \\ & 1/\tilde{\kappa}^2 & & O \\ & & \ddots & \\ & O & & 1/\tilde{\kappa}^{J-1} \\ & & & & 1/\tilde{\kappa}^J \end{bmatrix}. \tag{7.9}$$

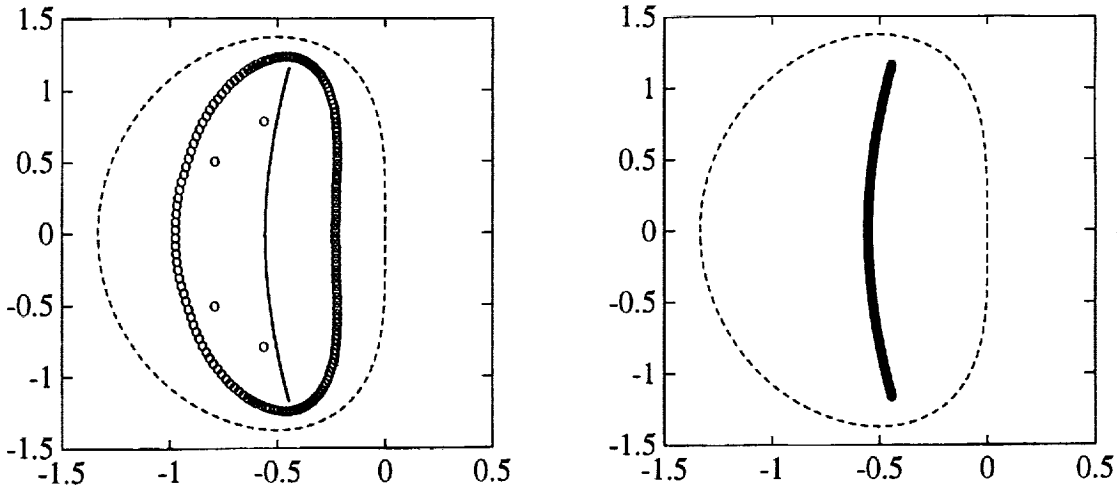

(a) $J = 160$ (b) $J = 160$

FIGURE 7.3. *Numerically computed spectra (o symbol) for (a) the unscaled Toeplitz matrix* $[-1/6, 1, -1/2, -1/3]$ *and (b) the scaled matrix. Asymptotic Toeplitz spectra and asymptotic circulant spectra indicated by "solid" and dashed lines respectively.*

Hence the rescaled eigenvalue problem is

$$(\mathbf{S}^{-1}\mathbf{A}\mathbf{S})\mathbf{S}^{-1}\boldsymbol{\phi} = \lambda\mathbf{S}^{-1}\boldsymbol{\phi}. \tag{7.10}$$

If $a_{ij} = a_{j-i}$ are the nonzero elements of the Toeplitz matrix $\mathbf{A}$, the elements $\tilde{a}_{ij}$ of the rescaled matrix $\mathbf{S}^{-1}\mathbf{A}\mathbf{S}$ are

$$\tilde{a}_{ij} = a_{j-i}\tilde{\kappa}^{j-i}. \tag{7.11}$$

To numerically compute the eigenvalues of the rescaled eigenvalue problem, one simply replaces the matrix elements by (7.11). One should not make the *numerical* matrix multiplies indicated by $\mathbf{S}^{-1}\mathbf{A}\mathbf{S}$ because of potentially large roundoff errors. The implementation of algorithm 4.1 in the Appendix computes $\hat{\kappa}(\psi)$ which can be used to compute (7.7).

In Fig. 7.3 we compare the computed (MATLAB) eigenvalues of the scaled and unscaled Toeplitz matrix defined by (7.1). One can predict a bound on the numerical eigenvalue distribution of a Toeplitz matrix for large J. In Fig. 7.4a the outer dashed line is the circulant cousin spectrum of the Toeplitz matrix defined by (7.1) and the inner dashed line is the circulant cousin of the corresponding *scaled* Toeplitz matrix. The solid line is the asymptotic Toeplitz spectrum. For the unscaled matrix the outer dashed line of Fig. 7.4a is the bound on the numerically computed eigenvalues for large J. For the scaled matrix, the inner dashed line is the asymptotic bound on the numerically computed eigenvalues. For the scaled matrix the circulant spectrum is tightly "wound" around the asymptotic Toeplitz spectrum and one can expect an accurately computed spectrum for large J. These bounds are illustrated by the numerical spectra shown in Figs. 7.3.

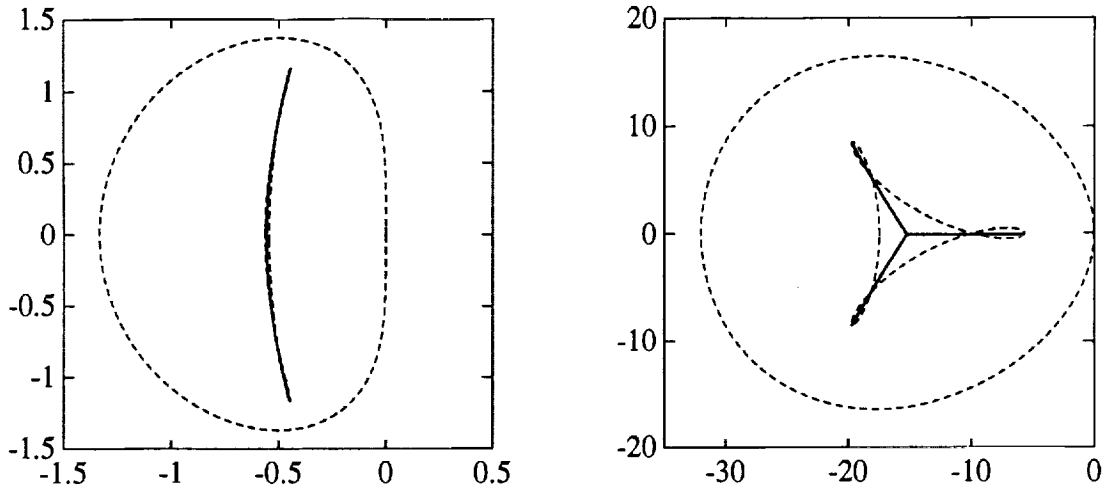

(a) $[-1/6, 1, \underline{-1/2}, -1/3]$ (b) $[-1.5, 16, \underline{-15}, 0, .5]$

FIGURE 7.4. *Asymptotic circulant spectra for unscaled ("outer" dashed lines) and scaled ("inner" dashed lines) matrices. Asymptotic Toeplitz spectra are indicated by "solid" lines.*

As a second example, we plot in Fig. 7.4b the spectra of the unscaled and scaled circulant cousins of the pentadiagonal Toeplitz matrix defined by

$$[-1.5, 16, \underline{-15}, 0, .5]. \tag{7.12}$$

The "solid line", i.e., the *propeller*, is the asymptotic Toeplitz spectrum. Numerically computed (MATLAB) spectra of the Toeplitz matrix and its transpose are plotted in Fig. 7.5a,b for $J = 400$. The eigenvalues for both $\mathbf{A}$ and $\mathbf{A}^T$ are erroneous for large J. The inner dashed curve of Fig. 7.4b is the asymptotic bound on the numerical eigenvalue distribution of the scaled matrix for large J. Numerical eigenvalue computations for the scaled matrix are shown in Fig. 7.5c,d.

One can also predict how "well" the scaling will work. If a graph of $|\hat{\kappa}|$ vs ψ_ℓ (see algorithm 4.1) for the unscaled matrix is a single "flat" band as in Fig. 7.2 then the scaling will yield a tight bound for the circulant cousin around the asymptotic Toeplitz spectrum as illustrated in Fig. 7.4a. On the other hand, if $|\hat{\kappa}|$ vs ψ_ℓ forms multiple and/or nonuniform bands as illustrated in Fig. 7.6, then one has multiple scales and a simple scaling will not yield a closely wound circulant cousin spectrum as illustrated in Fig. 7.4b.

If one starts with a quasi-Toeplitz matrix, then the appropriate scaling is the same as for its pure Toeplitz cousin.

8. The generalized eigenvalue problem. If Padé type difference approximations are used to approximate differential equations the associated stability analysis leads to the generalized eigenvalue problem. In addition, the analysis of implicit time integration schemes leads to a generalized eigenvalue problem. Let $\mathbf{A}$ and $\mathbf{B}$ represent $J \times J$ banded Toeplitz matrices. The generalized eigenvalue problem is defined by

$$\mathbf{A}\boldsymbol{\phi} = \lambda \mathbf{B}\boldsymbol{\phi} \tag{8.1}$$

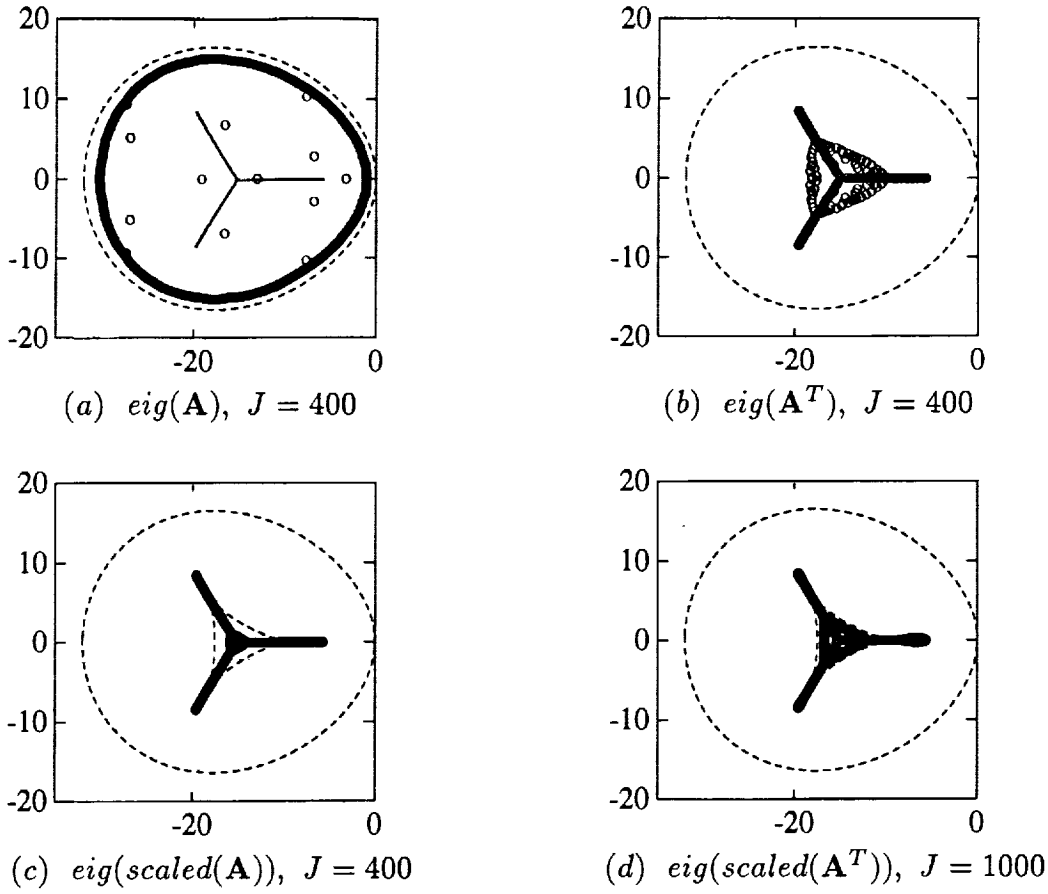

FIGURE 7.5. *Numerically computed spectra (o symbols) for (a)* $\mathbf{A} = [-1.5, 16, \underline{-15}, 0, .5]$, *(b)* $\mathbf{A}^T$, *(c) scaled* $\mathbf{A}$, $J = 400$, *and (d) scaled* $\mathbf{A}^T$, $J = 1000$.

where ϕ is the eigenvector and λ is the eigenvalue. Here we assume that the matrix $\mathbf{A}$ is defined by the sequence $[a_i, -p_A \leq i \leq q_A]$ and $\mathbf{B}$ is defined by the sequence $[b_i, -p_B \leq i \leq q_B]$ where p_A, q_A, p_B, q_B are positive integers. The indexing of the eigenvector ϕ is given by

$$\phi^T = [\phi_1, \phi_2, \cdots, \phi_{J-1}, \phi_J]. \tag{8.2}$$

The eigenvalue problem (8.1) is equivalent to the set of homogeneous difference equations

$$\sum_{m=-p_A}^{q_A} a_m \phi_{j+m} = \lambda \sum_{m=-p_B}^{q_B} b_m \phi_{j+m}, \quad j = 1, 2, \cdots, J \tag{8.3}$$

with $p = \max[p_A, p_B]$ homogeneous boundary conditions at the left boundary and $q = \max[q_A, q_B]$ homogeneous boundary conditions at the right boundary :

$$\phi_{-m} = 0, \quad m = 0, 1, \cdots, p-1, \qquad \phi_{J+m} = 0, \quad m = 1, 2, \cdots, q. \tag{8.4a,b}$$

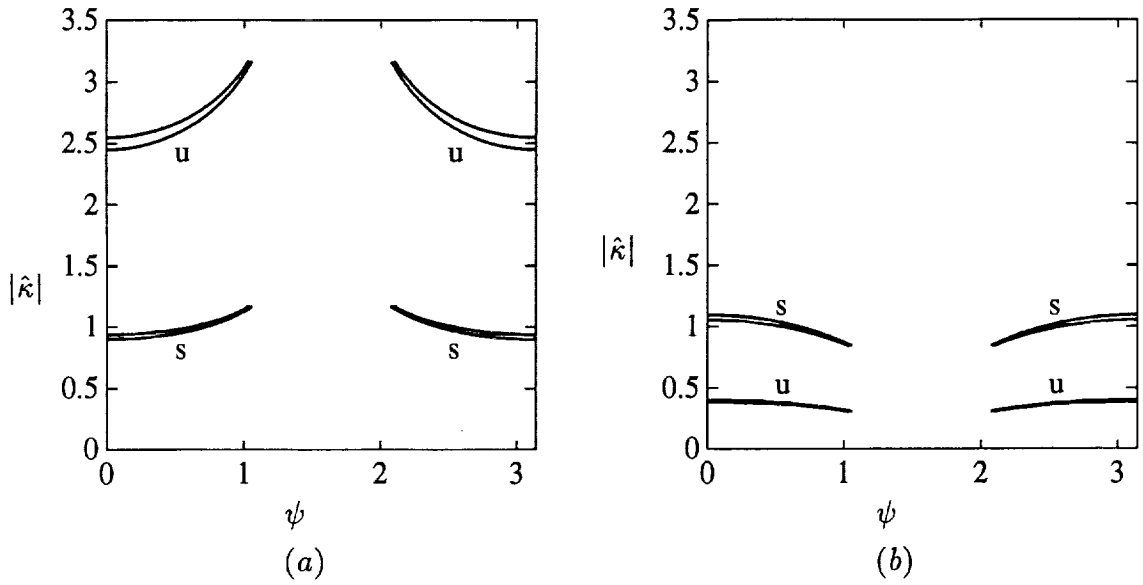

FIGURE 7.6. *Modulus of $\hat{\kappa}$ vs ψ_ℓ for (a) matrix $[-1.5, 16, \underline{-15}, 0, .5]$ unscaled, u, and scaled, s, and (b) the transpose matrix unscaled, u, and scaled, s.*

Equation (8.3) is a $(p+q)$-th order difference equation for ϕ_j and we look for a solution of the form

$$\phi_j = \kappa^j \tag{8.5}$$

where κ is a complex constant. Substitution of (8.5) into (8.3) yields

$$\lambda \sum_{m=-p_B}^{q_B} b_m \kappa^m = \sum_{m=-p_A}^{q_A} a_m \kappa^m. \tag{8.6}$$

This is an algebraic equation of degree $p+q$ in the unknown κ and we assume the roots are distinct. The general solution of (8.3) is

$$\phi_j = \sum_{m=1}^{p+q} \beta_m \kappa_m^j \tag{8.7}$$

where the β_m's are arbitrary constants. The constants β_m are determined by inserting (8.7) into the boundary conditions (8.4). If the bandwidth is three, i.e., $p = q = 1$, the eigenvalue problem for the pure Toeplitz problem can be solved analytically [15]. However, if the bandwidth is greater than three, the problem is analytically intractable.

The eigenvalue problem for the circulant cousin of (8.1) is (8.3) with periodic boundary conditions (2.12). Insertion of (8.5) into (2.12) yields

$$\kappa^J = 1. \tag{8.8}$$

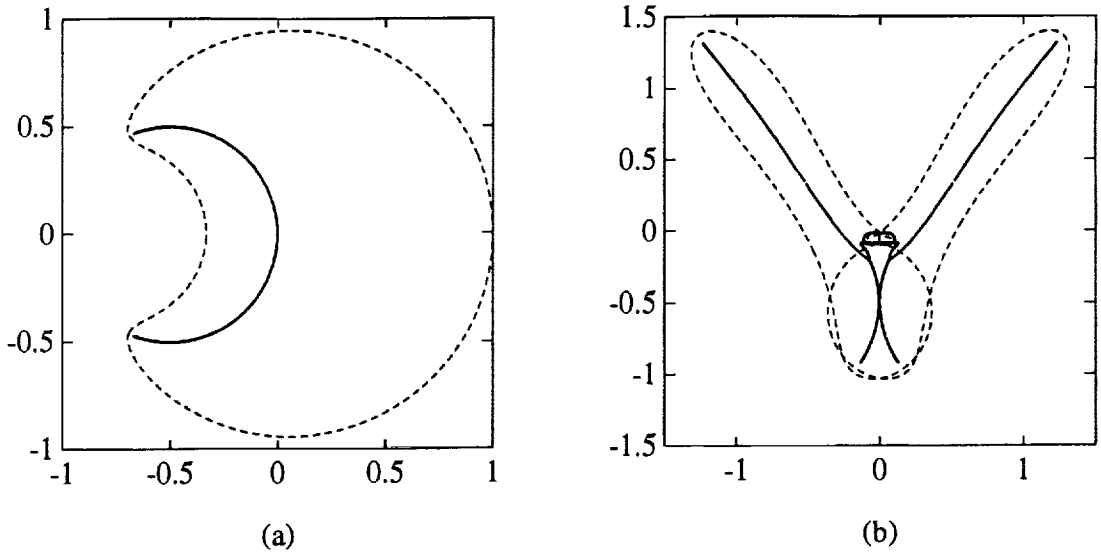

FIGURE 8.1. *Spectra for the generalized Toeplitz eigenvalue problem (8.1), (a)* $\mathbf{A} = [2, \underline{0}, -1]$ *and* $\mathbf{B} = [-2, \underline{2}, 1]$ *and (b)* $\mathbf{A} = [.38, .13, -.43, .15, \underline{.25}, -.06, .27, -.02, -.26]$ *and* $\mathbf{B} = [.28i, .38i, .50i, .07i, \underline{.95i}, .99i, .49i, .27i, .09i]$.

Hence the κ's are the J roots of unity given by (2.14) and the circulant spectrum is obtained by substituting (2.14) into (8.6):

$$\lambda_\ell \sum_{m=-p_B}^{q_B} b_m e^{im\theta_\ell} = \sum_{m=-p_B}^{q_B} a_m e^{im\theta_\ell}. \tag{8.9}$$

The partition of the spectrum for the asymptotic Toeplitz spectrum is the same (Section 3) as for the standard eigenvalue problem. The algorithm follows that of Section 4.1. To construct the polynomial for κ's of equal modulus we use (4.1). Since κ_a and κ_b (defined by 4.1) must each give the same value of λ when inserted in (8.6), we can eliminate λ and obtain a polynomial in $\hat{\kappa}$ with coefficients which are functions of the Toeplitz matrix coefficients and ψ_ℓ. In particular,

$$\lambda(\kappa_a) \sum_{m=-p_B}^{q_B} b_m \hat{\kappa}^m e^{im\psi_\ell} = \sum_{m=-p_A}^{q_A} a_m \hat{\kappa}^m e^{im\psi_\ell} \tag{8.10a}$$

$$\lambda(\kappa_b) \sum_{m=-p_B}^{q_B} b_m \hat{\kappa}^m e^{-im\psi_\ell} = \sum_{m=-p_A}^{q_A} a_m \hat{\kappa}^m e^{-im\psi_\ell} \tag{8.10b}$$

and since

$$\lambda(\kappa_a) = \lambda(\kappa_b) \tag{8.11}$$

one obtains, after some algebraic simplification,

$$\sum_{m=-p_A}^{q_A} \sum_{n=-p_B}^{q_B} a_m b_n \hat{\kappa}^{(m+n)} \sin[(m-n)\psi_\ell] = 0. \tag{8.12}$$

The algorithm follows that of (i) and (ii) in Section 4.1. The implementation of the generalized eigenvalue algorithm is a straightforward modification of the standard eigenvalue algorithm (Appendix).

As an example of the $\hat{\kappa}$ polynominal (8.12), if we choose **A** and **B** to be the quadridiagonal matrices represented by the sequences $[a_{-2}, a_{-1}, a_0, a_1]$ and $[b_{-2}, b_{-1}, b_0, b_1]$,respectively, the equation for the κ's of equal modulus is

(8.13)

$$\begin{aligned}(a_1 b_0 - a_0 b_1)\hat{\kappa}^4 + 2(a_1 b_{-1} - a_{-1} b_1)\cos(\psi_\ell)\hat{\kappa}^3 + \\ [(a_0 b_{-1} - a_{-1} b_0) + (a_1 b_{-2} - a_{-2} b_1)(4\cos^2(\psi_\ell) - 1)]\hat{\kappa}^2 + \\ 2(a_0 b_{-2} - a_{-2} b_0)\cos(\psi_\ell)\hat{\kappa} + (a_{-1} b_{-2} - a_{-2} b_{-1}) = 0.\end{aligned}$$

Note that (6.4) and the "transpose" of (6.25) are easily obtained as special cases of (8.13). As examples of the spectra of the generalized eigenvalue problem we choose two examples. The spectra for the Toeplitz and the associated circulant Toeplitz matrices are plotted in Fig. 8.1

9. Concluding Remarks. The algorithms presented in Section 4 provide a practical accurate method for obtaining the asymptotic spectra of banded Toeplitz and quasi-Toeplitz matrices. They are especially useful for non-normal matrices where conventional algorithms may give erroneous results. The extension of the algorithms for the generalized eigenvalue problem for Toeplitz matrices was presented in Section 8. The asymptotic analysis also provides a similarity transformation, Section 7, which can increase the spectrum accuracy if conventional eigenvalue algorithms are employed.

Acknowledgements. We are grateful to Dennis Jespersen, Robert Schreiber, and Nick Trefethen for comments and suggestions which improved our manuscript.

Appendix. MATLAB Toeplitz eigenvalue algorithm.

```
function[teig, spsi, sakap] = toeasy(c, r, nn);
%Find the asymptotic (size approaches infinity) spectrum
%for a banded Toeplitz matrix with first column 'c' and first row
%'r' (only banded part of column and row) nn is a measure of the
% number of points computed on the spectrum
diag = c(1);
lr = length(r);
nr = lr - 1;
lc = length(c);
nc = lc - 1;
ct = c(2 : lc);
```

```
rt = r(2 : lr);
mv = nr : -1 : -nc;
pc0 = [fliplr(rt) 0 ct];
teig = [1 : (nc + nr) * nn];
spsi = [1 : (nc + nr) * nn];
sakap = [1 : (nc + nr) * nn];
eigct = 0;
epst = 1000 * eps;
for j = 1 : nn;
 psi = j * pi/(nn + 1);
 mvs = sin(mv * psi);
 pe = pc0. * mvs;
 nroot = nc + nr;
 if (pe(2) ~= 0);
  if(abs(pe(1)/pe(2)) < 1000 * eps);
   pe = pe(2 : nroot + 1);
   nroot = nroot - 1;
  end;
 end;
 ke = roots(pe);
 for k = 1 : nroot;
 if ke(k) ~= 0;
  kap = ke(k) * exp(i * psi);
  lam = -(kap. ^ mv) * pc0.';
  pc = [fliplr(rt) lam ct];
  kc = roots(pc);
  akap = abs(kap);
  akc = abs(kc);
  skap = sort(akc);
  test = abs((skap(nc) - skap(nc + 1))/(skap(nc) + skap(nc + 1)));
  if test < epst&skap(nc) > akap * (1 - epst)&skap(nc) < akap * (1 + epst);
   eigct = eigct + 1;
   teig(eigct) = -(lam - diag);
   spsi(eigct) = psi;
   sakap(eigct) = akap;
  end;
 end;
end;
end;
teig = teig(1 : eigct);
spsi = spsi(1 : eigct);
sakap = sakap(1 : eigct);
```

REFERENCES

[1] P. J. Davis, "Circulant Matrices," John Wiley, New York, 1979.

[2] S. K. Godunov, V. S. Ryabenkii, *Special stability criteria of boundary value problems for non-selfadjoint difference equations*, Russ. Math. Surv. **18** (1963), 1–12.

[3] G. H. Golub and C. F. Van Loan, "Matrix Computations," Second Edition, Johns Hopkins University Press, Baltimore, 1989.

[4] R. M. Gray, *On the asymptotic eigenvalue distribution of Toeplitz matrices*, IEEE Trans. Info. Theory **18** (1972), 725-730.

[5] U. Grenander and G. Szegö, "Toeplitz Forms and Their Applications," Univ. of California Press, Berkeley, 1958.

[6] B. Gustafsson, H.-O. Kreiss, and A. Sundström, *Stability theory of difference approximations for mixed initial boundary value problems. II*, Math. Comp. **26** (1972), 649–686.

[7] H.-O. Kreiss, *Stability theory for difference approximations of mixed initial boundary value problems*, Math. Comp. **22** (1968), 703-714.

[8] L. Reichel, L. N. Trefethen, *Eigenvalues and pseudo-eigenvalues of Toeplitz Matrices*, to appear in Lin. Alg. Applics.

[9] P. Schmidt and F. Spitzer, *The Toeplitz matrices of an arbitrary Laurent Polynomial*, Math. Scand. **8** (1960), 15–38.

[10] G. D. Smith, "Numerical Solution of Partial Differential Equations: Finite Difference Methods," Second Edition, Oxford University Press, Oxford, 1978.

[11] J. C. Strikwerda, *Initial boundary problems for the method of lines*, J. Comp. Phys. **34** (1980), 94–107.

[12] L. N. Trefethen, *Non-Normal Matrices and Pseudospectra*, book in preparation.

[13] J. L. Ullman, *A problem of Schmidt and Spitzer*, Bull. Amer. Math. Soc. **73** (1967), 883-885.

[14] R. F. Warming and R. M. Beam, *An eigenvalue analysis of finite-difference approximations for hyperbolic IBVPs II: the auxiliary Dirichlet problem*, in "Third International Conference on Hyperbolic Problems, Vol II," B. Engquist and B. Gustafsson, eds., Studentlitteratur, Lund, 1991, pp. 923–937.

[15] R. F. Warming and R. M. Beam, *The generalized eigenvalue problem for tridiagonal Toeplitz Matrices*, to appear.

REPORT DOCUMENTATION PAGE

Form Approved
OMB No. 0704-0188

1. AGENCY USE ONLY *(Leave blank)*	2. REPORT DATE	3. REPORT TYPE AND DATES COVERED
	November 1991	Technical Memorandum

4. TITLE AND SUBTITLE
The Asymptotic Spectra of Banded Toeplitz and Quasi-Toeplitz Matrices

5. FUNDING NUMBERS
505-59-53

6. AUTHOR(S)
Richard M. Beam and Robert F. Warming

7. PERFORMING ORGANIZATION NAME(S) AND ADDRESS(ES)
Ames Research Center
Moffett Field, CA 94035-1000

8. PERFORMING ORGANIZATION REPORT NUMBER
A-92006

9. SPONSORING/MONITORING AGENCY NAME(S) AND ADDRESS(ES)
National Aeronautics and Space Administration
Washington, DC 20546-0001

10. SPONSORING/MONITORING AGENCY REPORT NUMBER
NASA TM-103900

11. SUPPLEMENTARY NOTES
Point of Contact: Richard M. Beam, Ames Research Center, MS 202A-1, Moffett Field, CA 94035-1000
(415) 604-5895 or FTS 464-5895

12a. DISTRIBUTION/AVAILABILITY STATEMENT
Unclassified — Unlimited
Subject Category 64

12b. DISTRIBUTION CODE

13. ABSTRACT ***(Maximum 200 words)***

Toeplitz matrices occur in many mathematical as well as scientific and engineering investigations. This paper considers the spectra of *banded* Toeplitz and *quasi*-Toeplitz matrices with emphasis on non-normal matrices of arbitrarily large order and relatively small bandwidth. These are the type of matrices that appear in the investigation of stability and convergence of difference approximations to partial differential equations. Quasi-Toeplitz matrices are the result of non-Dirichlet boundary conditions for the difference approximations. The eigenvalue problem for a banded Toeplitz or quasi-Toeplitz matrix of large order is, in general, analytically intractable and (for non-normal matrices) numerically unreliable. An asymptotic (matrix order approaches infinity) approach partitions the eigenvalue analysis of a quasi-Toeplitz matrix into two parts, namely the analysis for the boundary condition *independent* spectrum and the analysis for the boundary condition *dependent* spectrum. The boundary condition independent spectrum is the same as the *pure* Toeplitz matrix spectrum. Algorithms for computing both parts of the spectrum are presented. Examples are used to demonstrate the utility of the algorithms, to present some interesting spectra, and to point out some of the numerical difficulties encountered when conventional matrix eigenvalue routines are employed for non-normal matrices of large order. The analysis for the Toeplitz spectrum also leads to a diagonal similarity transformation that improves conventional numerical eigenvalue computations. Finally, the algorithm for the asymptotic spectrum is extended to the Toeplitz generalized eigenvalue problem which occurs, for example, in the stability analysis of Padé type difference approximations to differential equations.

14. SUBJECT TERMS
Toeplitz matrices, Eigenvalues, Spectrum, Stability

15. NUMBER OF PAGES
38

16. PRICE CODE
A03

17. SECURITY CLASSIFICATION OF REPORT	18. SECURITY CLASSIFICATION OF THIS PAGE	19. SECURITY CLASSIFICATION OF ABSTRACT	20. LIMITATION OF ABSTRACT
Unclassified	Unclassified		